Understanding changes in plant productivity using EVI satellite data in Tswalu Kalahari Reserve

Wataru Tokura

Supervisor: Prof. Timm Hoffman
Co-supervisors: Sam Jack and Tania Anderson

Submitted in partial fulfilment of the requirements for the degree of Master of Science in Conservation Biology in coursework and dissertation

Percy FitzPatrick Institute of African Ornithology
Department of Biological Sciences
University of Cape Town, Rondebosch, 7701 South Africa

February 2016

Plagiarism Declaration

I know the meaning of plagiarism and declare that all of the work in the dissertation, save for that which is properly acknowledged, is my own.

Signed: Signed ______________________

Date: 12th of February 2016

Table of Contents

Acknowledgements

I would like to thank my supervisors, Prof. Timm Hoffman, Mr Sam Jack, and Ms Tania Anderson for their guidance and advice. A special thanks to A/Prof Julian Smit (Faculty of Engineering & the Built Environment, UCT), Mr Christiaan J. Harmse (Department of Agriculture, Land Reform and Rural Development, Northern Cape Province), Ms Clair Davis (CSIR), and Ms Feroza Morris (University of KwaZulu-Natal) for technical advice. Parts of the rainfall record used for analysis were provided by the South African Weather Services. I also would like to thank Mr Bonginkosi Prince Ngomane, Mr Armin du Plessis, and Ms Kelsey Green for assisting with my field work, as well as Mr Dylan Smith (Tswalu Kalahari Reserve) and Tswalu Kalahari Reserve for providing data and enabling this research.

Abstract

In the arid African savanna, the limited availability of water strongly affects plant productivity, but other key drivers of vegetation dynamics, such as herbivory and fire, are usually considered to have a relatively minor impact. The main purpose of this study was to characterise the spatial and temporal pattern in plant productivity in the 100 000 hectare Tswalu Kalahari Reserve (TKR) in the semi-arid Northern Cape and relate the observed changes to potential drivers using medium spatial resolution of MODIS Enhanced Vegetation Index (EVI) time series data (16 day, 250 m) from 2000 to 2015.

The time series of EVI for the past 16 years in TKR presented a highly seasonal pattern which fluctuated between years. A composite of annual small integrated value of EVI images highlighted spatial and temporal heterogeneity of plant productivity in the area. The EVI value was mainly influenced by rainfall and effect of fire and herbivory was considered to be minor. These observations confirmed the extreme variability of plant productivity in the drylands in the summer rainfall region of South Africa. Additionally, most of the values concerning the phenometrics of EVI differ significantly among vegetation types. This suggests that the structure and function of the vegetation determine plant productivity as well as their being a possible effect of soil property and reflectance. The trend in plant productivity computed by residual trend analysis (RESTREND) detected a significant positive trend in plant productivity in the east and south west of TKR, which overlapped with shrub-dominated vegetation, providing evidence for possible ongoing bush encroachment in these areas. On the other hand, a negative trend was detected in some locations in the west. The data generated from MODIS EVI and the small integrated value of EVI using TIMESAT produced biologically interpretable results. However, the correlative relationship between the EVI derived from Landsat Operational Land Imager (OLI) and plant cover estimated in the field was poor or not significant and needs to be examined further.

The information obtained from this project will help to guide reserve management. The extreme variability of plant productivity needs to be considered when making management decisions. Also, areas where change was detected require further study including validation of the satellite derived data, field based species level surveys, and a long-term, ground-based vegetation monitoring.

1 Introduction

1.1 The Dynamics of Vegetation and Degradation in Semi-arid Regions

In drylands, the limited availability of water strongly affects plant productivity. This has led to the 'pulse-reserve' theory for dryland dynamics (Schwinning et al. 2004; Wessels et al. 2007; Wistebaar 2008; Collins et al. 2014). This theory suggests that rainfall triggers a pulse of vegetation growth which in turn results in a reserve of carbon and energy in the form of organic matter. These relationships are influenced by the timing and amount of rainfall, as well as soil type and the plant functional groups present (Reynolds et al. 2004). Other key drivers of vegetation dynamics, such as herbivory and fire, are usually considered to have a relatively minor impact on dryland ecosystem dynamics because their impacts are thought to be masked by the erratic rainfall which characterises dryland environments. The non-equilibrium concept of rangelands suggests that where rainfall variability is high, degradation caused by herbivory is relatively low because herbivore populations collapse during drought (von Wehrden et al. 2012). Likewise, a meta-analysis of the key drivers of African savanna dynamics indicated that disturbances such as fire and herbivory rarely regulate woody plant cover where mean annual rainfall is below 350 mm (Sankaran et al. 2005).

However, even in areas with high rainfall variability degradation may occur if water and other key resources such as supplemental fodder are available during periods of drought, because herbivores can utilise these resources (von Wehrden et al. 2012). Indeed, many studies have indicated degradation caused by overgrazing in rangelands in arid and semi-arid regions. Vegetation change, bush encroachment, and soil erosion are all examples of the consequences of rangeland degradation due to excessive grazing pressure (Hoffman & Todd 2000; Tongway et al. 2003; Gillson & Hoffman 2007; Han et al. 2008; Wistebaar 2008).

Processes of change in species composition and vegetation structure due to the introduction of livestock farming have been documented. For example, Parsons et al. (1997) reported a difference in vegetation structure and function between game reserves, commercial livestock farms, and communal lands in semi-arid north-western South Africa. An experimental study showed increased shrub abundance following the introduction of a high density of livestock in western Botswana (Skarpe 1990). Wasiolka & Blaum (2011) compared species richness and plant cover between a protected area and several livestock farms in the southern Kalahari, and found higher shrub cover but a lower proportion of perennial grass cover, herb cover and herb species richness in the livestock farms. Comparison of rangeland condition across six sites in the arid and semi-arid regions in South Africa confirmed the effect of heavy grazing on species composition that often resulted in a decrease in foraging quality of grass and an increase in annual species (Rutherford & Powrie 2013).

These findings imply that there is a direct, density-dependent influence of herbivory on vegetation due to a change in feeding behaviour and intensity of grazing in drylands. As suggested by Hempson et al. (2015), rainfall and herbivory interact to determine the dynamics of plant productivity in arid and semi-arid rangelands and trajectories of vegetation change will vary in response to land use impacts.

1.2 The Use of Remote Sensing Data for Monitoring Dryland Environments

Understanding the spatial pattern and process of how land use effects the environment is one of the key questions in landscape ecology. Improved accessibility to remote sensing data and analytical software packages have enabled long-term and large-scale ecological monitoring, including land use change, plant productivity, and fire activity (e.g. Palmer & Fortescue 2004; Pettorelli et al. 2005; Pfeifer et al. 2012; Lausch et al. 2013). In particular, vegetation indices (VI) derived from satellite Earth Observation (EO) data have been used in a number of studies because of their direct correlation with plant productivity (Pettorelli et al. 2005). Examples of the applications of VI include the monitoring of net primary production (NPP) to evaluate the long-term trend of plant productivity (Fensholt & Rasmussen 2011; Sjöström et al. 2011; Davis 2012; Mbow et al. 2013), to assessments of degradation (Wessels et al. 2007, 2008; Wistebaar 2008; Fensholt et al. 2013; Eckert et al. 2015), to detection of vegetation change (Palmer & van Rooyen 1998; Jamali et al. 2014; Dubovyk et al. 2015), and to mapping and the description of biomes (Wessels et al. 2011). Recently, a growing number of studies have employed Leaf Area Index (LAI) and fractional Photosynthetically Active Radiation (fPAR) developed from EO data for similar purposes, including to understand and model plant productivity (Palmer & Yunusa 2011; Palmer et al. 2015) and to assess degradation (Bennett et al. 2012). EO data, with its extensive spatial coverage and historical archives, can provide crucial information for ecosystem management which circumvent the logistical challenges of conventional, field-based techniques.

However, the use of EO data for monitoring vegetation in arid and semi-arid area has its own set of challenges. Firstly, the Normalised Difference Vegetation Index (NDVI), which is the most commonly used VI, is sensitive to the background 'noise' generated by the soil, particularly in the sparsely vegetated environments which characterise many arid and semi-arid areas (Huete et al. 2002; Pettorelli et al. 2005). To overcome this weakness, several alternative vegetation indices have been developed for drylands (see methods for details). Secondly, to isolate the influence of drivers other than rainfall (i.e. human-induced land degradation) is challenging, because plant productivity is strongly influenced by the erratic rainfall of dryland environments (Wessels et al. 2007; Davis 2012). Several techniques have been developed to identify anthropogenic impacts by removing the effect of rainfall, such as Rain-use efficiency (RUE) (Wessels et al. 2007; del Barrio et al. 2010; Fensholt & Rasmussen 2011) and residual trend analysis (RESTREND) (Wessels et al. 2007, 2012; Davis 2012), but their application has met with mixed success. Another difficulty occurs in interpreting the outcome of trend analysis. Because these EO data-based techniques define degradation as a change in plant productivity, the change that is detected does not always correspond to change in species or functional types (van Rooyen 2000). Therefore, selecting appropriate indices and techniques, as well as understanding the capabilities and limitations of EO data is necessary for vegetation monitoring in arid and semi-arid regions. Furthermore, an understanding of the ecology and vegetation dynamics of the region in response to rainfall and herbivory is also important as this helps in the interpretation of the patterns exhibited in the EO data.

1.3 Vegetation and Degradation in the Kalahari

The Kalahari is a generally flat and dry, sand-dominated area located in the interior of central and southern Africa. Broadly, the vegetation is classified as savanna, covered with a limited number of species of grass, shrubs and sparse trees (van Rooyen & van Rooyen 1998). The land surface is dominated by aeolian soil of low nutrient status (Wang et al. 2007). Annual rainfall is highly erratic but over 80% falls between October and April (Sporton & Thomas 2002). The occurrence and impact of fire is spatially heterogeneous but occurs least in the driest southwestern region of the Kalahari and increases with rainfall (van der Walt & le Riche 1984; Thomas & Paul 1991).

Although the Kalahari is a hot and dry climate for humans, archaeological evidence suggests that there has been a long history of people in the region dating back to the Early Stone Age >100,000 years BP. It is assumed, however, that human impact on the environment was not significant before the arrival of domestic animals in the region ca. 2000 years ago. Thereafter, as the human and livestock populations grew, their influence on the Kalahari environment is thought to have increased while exploitation expanded rapidly following the establishment of trading routes with European settlements to the south and east of the region from the 19th century onwards (Sporton & Thomas 2002). In the nineteenth century, the area experienced major changes in land use and the adverse effect on the environment became apparent. This included a decrease in the number of large mammals including elephants and rhinos, the spread of cattle farming enabled by the establishment of permanent wells, a reduction of surface water and wetland environments, and a change in vegetation most notably an increase in woody shrubs and trees, a phenomenon known as bush encroachment (Thomas & Paul 1991).

Today, livestock farming is one of the major industries in the southern Kalahari, and the area is comprised largely of fenced rangelands with a few large protected areas (Sporton & Thomas 2002). The degradation of rangelands caused by selective overgrazing has been a major concern in the region, because of its potential negative impact on carrying capacity and productivity. Degraded rangelands typically shift from being dominated by perennial grasses to unpalatable woody species, or in some cases to annual grass species only. Previous research has shown that overgrazing facilitated an increase in shrub species such as *Rhigozum trichotomum* (van Rooyen 2000), *Crotalaria* cf. *spartioides* (Rutherford & Powrie 2009), and *Senegalia mellifera* and *Grewia flava* (Skarpe 1990), while several species of perennial grass became locally extinct, with a concomitant reduction in species richness (Rutherford & Powrie 2010). Additionally, the trampling of vegetation and the redistribution of nutrients by animals often causes degradation. For example, circular patterns of vegetation characterised by bare soil, annual plants, woody shrubs and grasses are often associated with the areas around artificial water point (Jeltsch et al. 1997a). Once degraded rangelands remain degraded for many years without human intervention, because the loss of vegetation cover triggers a positive feedback process which prevents recovery of the vegetation (Jeltsch et al. 1997b; van Rooyen 2000). In this sense, degradation of the Kalahari environment is irreversible and because of this the region should be considered sensitive to overgrazing.

1.4 The Use of Satellite Earth Observation data for Vegetation Studies in the Kalahari

Given the ecological and economic importance of rangelands, as well as the extensive spatial scale of the region, several studies have employed satellite EO data to monitor and assess veld condition in the central and southern Kalahari.

Earlier studies reported that satellite-derived NDVI may not be well correlated with the cover of vegetation as measured in the field. Palmer & van Rooyen (1998) found that the highest NDVI values were recorded in areas with contrasting amounts of vegetation cover. For example, high NDVI values were found in areas with high woody shrub cover as well as in areas with low grass cover such as on the crests of dunes. van Rooyen (2000) detected a significant negative correlation between plant cover and NDVI computed from Landsat TM. He argued that the high iron oxide content in the Kalahari sand was the cause of these perplexing trends and concluded that NDVI is not a reliable indicator of vegetation productivity in the Kalahari. However, a recent study used MODIS derived time-series NDVI data to understand vegetation dynamics in central Botswana and effectively outlined vegetation trends in relation to the potential drivers (Mishra et al. 2015a).

Furthermore, multispectral bands from Landsat data have also been successfully used to estimate vegetation cover. Thomas & Leason (2005) found a significant negative correlation between plant cover and TM3 reflectance values in the dry season in the Kgalagadi National Park in South Africa, and determined vegetation cover using this relationship. Ringrose & Matheson (1996) identified the extent of bare ground around rural villages in Botswana using multiband Landsat TM data. However, as for NDVI, identifying vegetation cover by contrasting 'green' and soil reflectance values using the red-infrared band is not reliable in sparse vegetation due to the noise from bare ground. Notwithstanding this problem, the use of multispectral bands did allow for the differentiation of reflectance values between different vegetation and land cover types (Thomas & Leason 2005).

More recently, the use of modified VI for sparsely vegetated arid and semi-arid areas, such as the soil adjusted vegetation index (SAVI) and the enhanced vegetation index (EVI), have shown encouraging results in several vegetation studies. For example, Hüttich et al. (2009) detected characteristic phenological patterns of plant productivity represented from MODIS EVI time series data in Namibia, but did not test the correlation between field measured vegetation cover and EVI. MODIS EVI time-series data used to characterise the phenological character of vegetation in South Africa (Colditz et al. 2007; Wessels et al. 2011), and the response of plant productivity following a rainfall event in the Okavango (Udelhoven et al. 2015), both produced biologically sensible results.

The above studies highlight the potential value but also the difficulties in using EO data for monitoring vegetation in the Kalahari environment. In particular, background noise from soil needs to be addressed to produce meaningful results. As is the case in other arid and semi-arid areas, adopting appropriate methodologies, as well as validating the reliability of the EO data through ground-truthing exercises is necessary for any work undertaken in the Kalahari.

1.5 Aims and Objectives

The main purpose of this study was to characterise the spatial and temporal pattern in plant productivity in the 100 000 hectare Tswalu Kalahari Reserve (TKR) in the semi-arid Northern Cape and relate the observed changes to potential drivers using EO data. The study in TKR provides a unique opportunity to investigate, through time-series data, the effect of a shift in management from livestock farming to herbivory by wild ungulates on the vegetation of the region.

The results of this study have direct implications for the management of TKR, as well as other reserves in the region, where a number of livestock farms have been converted into game reserves (Cousins et al. 2008). Furthermore, understanding the dynamics and evaluating the influence of different potential drivers has value for climate change studies since most climatic models have predicted that the Kalahari will experience an increase in aridity and will become significantly hotter and drier by 2100 (Thomas et al. 2005; Shongwe et al. 2009; Collins et al. 2013; Mishra et al. 2015a).

Specifically, this study aimed to answer the following questions:

- **Question 1.** How does vegetation productivity vary both temporally and spatially within the Tswalu Kalahari Reserve (TKR)? To answer this question, I produced a Landsat-based classification of the vegetation of TKR using remote sensing data and existing conceptual frameworks. I then developed a measure of vegetation productivity using phenological criteria and tracked the spatial change in this value through time for all areas within TKR.
- **Question 2.** What is the relationship between vegetation productivity and rainfall, fire, and vegetation type?
- **Question 3.** What are the patterns of degradation within TKR over the period 2001-2013 and how are these degradation trends reflected in the different vegetation types?
- **Question 4**. What are the implications of this study for the management of TKR?

2 Methods

2.1 Study Site

The Tswalu Kalahari Reserve (S -27.2031, E 22.4673) covering 1020 km^2, is situated approximately 160 km north-east of Upington in the Northern Cape Province, South Africa (Fig. 2.1). The climate is typically hot and arid, and the highly variable rainfall mainly occurs during summer from December to April. Mean annual rainfall for the past 25 years at the rain station Dedeben (S -27.2858, E 22.4850) was 361.4 ± 169.2 mm (South African Weather Service 2015). The area falls within the Savanna Biome, where the mean plant growth season starts in October and ends in June to August the following year (Wessels et al. 2011). The landscape is characterised by rocky mountains, sandy plains, and parallel-running sand dunes (Davis et al. 2010). TKR is dominated by the Korannaberg Mountains, which extend from north to south, through the middle of the reserve. The highest peak in the Korannaberg Mountains is Blou Krans, at 1580 m above sea level. Five different vegetation units are mapped by Mucina & Rutherford (2006) in the TKR. These include Koranna-Langeberg Mountain Bushveld, Gordonia Duneveld, Gordonia Plains Shrubveld, Olifantshoek Plains Thornveld, and Kathu Bushveld (Fig. 2.2). A more detailed vegetation study classified the region into 17 vegetation communities (van Rooyen et al. 2005).

Prior to 1995 TKR was split into more than 40 livestock farms, but was converted into a game reserve by removing fences, closing several artificial water points and restocking with indigenous animals that used to occur in the region (Davis et al. 2010). TKR has undergone continual expansion in the last 20 years. Today, 75 mammal species are present and the reserve has been developed into a luxury safari lodge. Most of the introduced mammals are grazing herbivores (e.g. Gemsbok *Oryx gazella*, Springbok *Antidorcas marsupialis*, Blue Wildebeest *Connochaetes taurinus*, and Hartebeest *Alcelaphus buselaphus*), with a lesser number of browser species (e.g. Greater Kudu *Tragelaphus strepsiceros*, Giraffe *Giraffa camelopardalis*, and Black Rhinoceros *Diceros bicornis*), omnivores (e.g. Chacma Baboon *Papio ursinus*), and predators (e.g. Leopard *Panthera pardus*, African Wild Dog *Lycaon pictus*). The reserve is divided into three areas by fences, which prevent medium- and large-sized mammals from moving across these areas unless guided by management personnel. The north eastern section of the reserve is designated as a “predator camp”, where Lions *Panthera leo* are present, while the north west corner of the reserve has been divided into separate camps for the breeding of Roan *Hippotragus equinus* and Sable antelope *Hippotragus niger*.

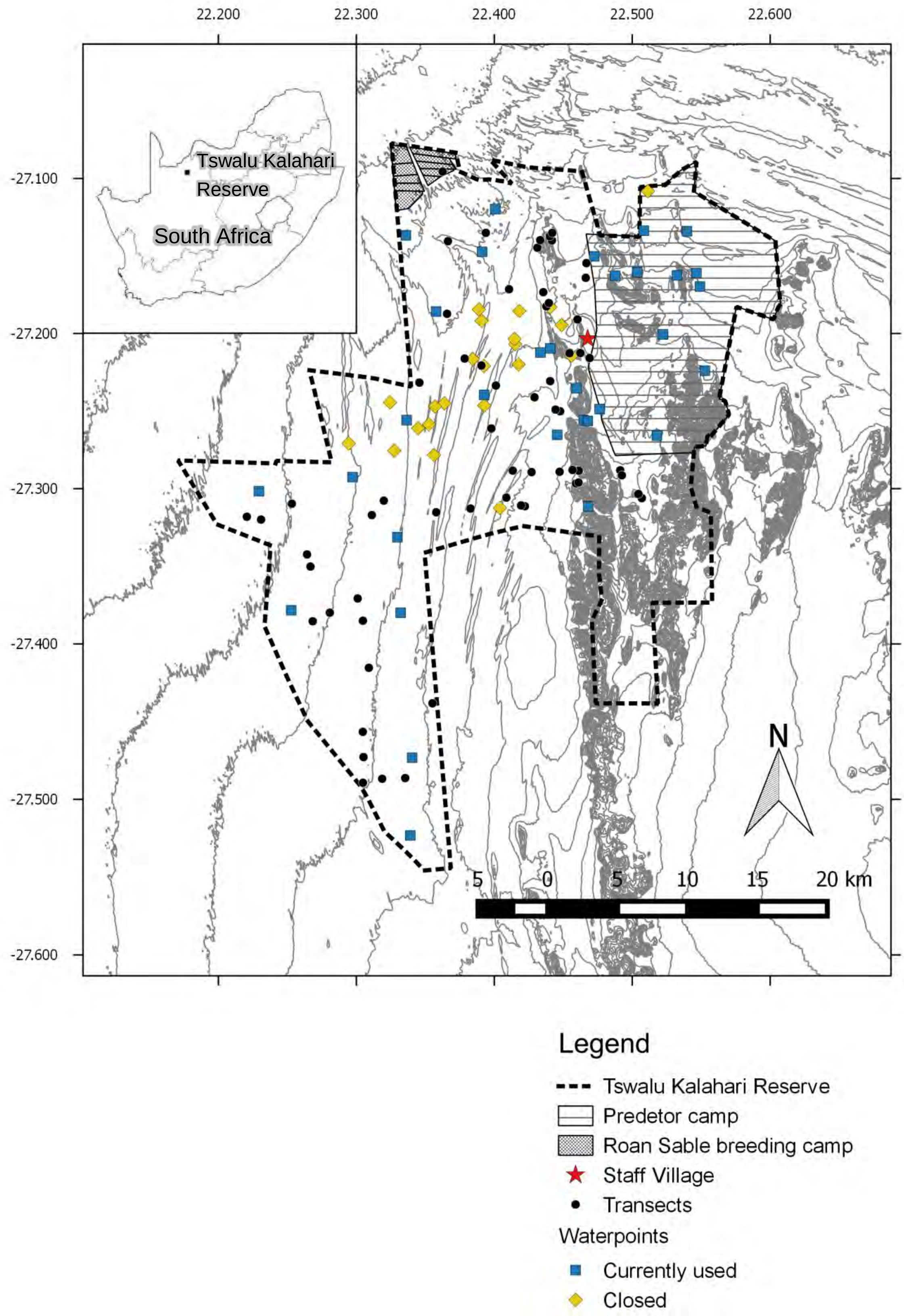

Fig. 2.1 Location of Tswalu Kalahari Reserve in the Northern Cape Province, South Africa. The black dots show the location of the transect surveys, and grey contours represent elevation.

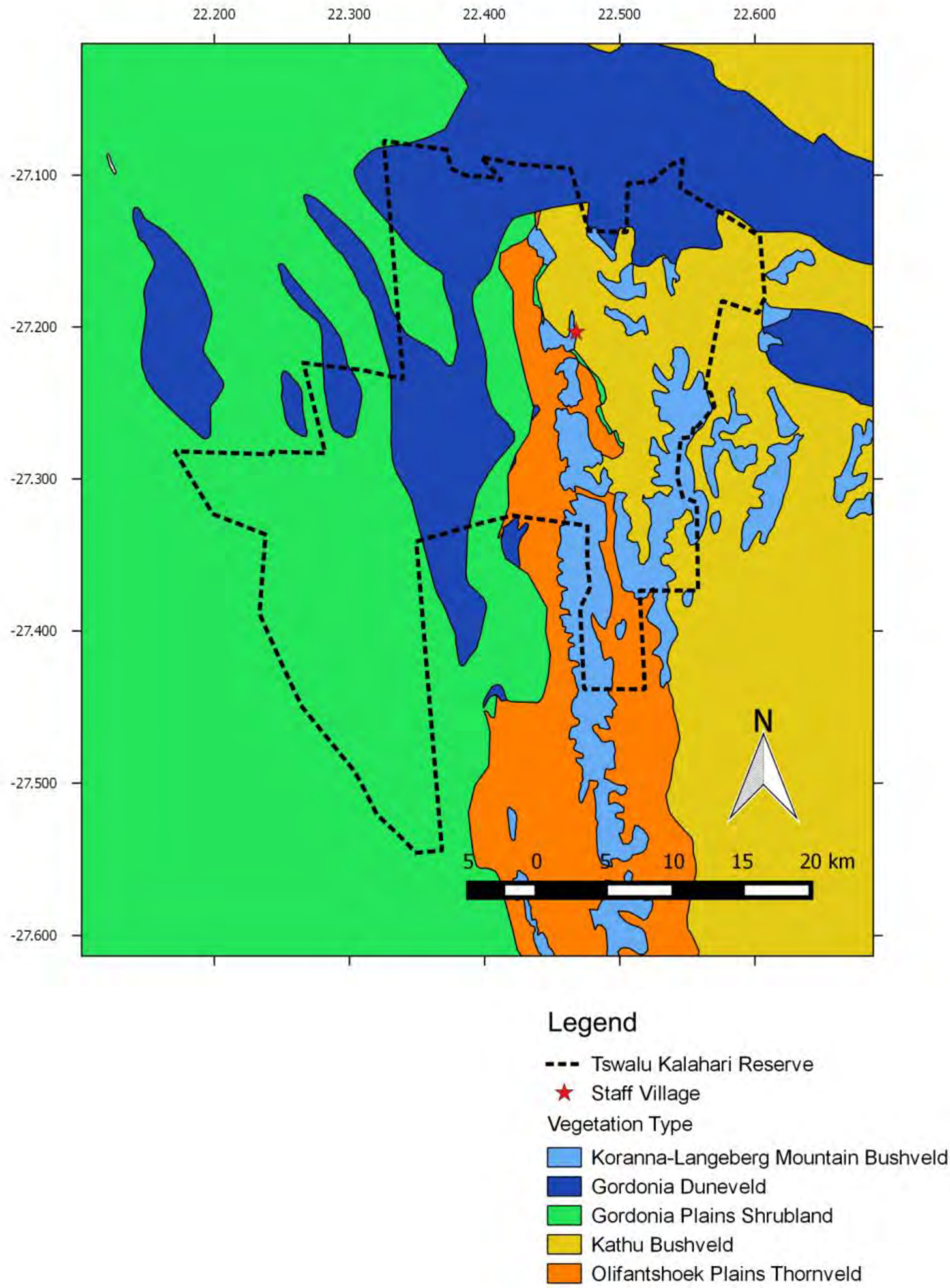

Fig. 2.2 Vegetation map of Tswalu Kalahari Reserve adapted from Mucina & Rutherford (2006).

2.2 Data

Satellite Based Vegetation Indices

The vegetation indices (VI) values derived from the Moderate Resolution Imaging Spectroradiometer (MODIS) were used as proxies for plant productivity. The MODIS sensor located on the satellite, Terra, has collected vegetation indices at 1 - 2 day intervals since February 2000 and 16-day composite products have been developed at 250 m, 500 m, and 1 km resolutions (Huete et al. 2002). During the development process, vegetation indices were corrected for atmospheric, soil, polarisation, and directional effects (Huete et al. 2002). The MODIS data produce two vegetation indices, the Normalised Difference Vegetation Index (NDVI) and the Enhanced Vegetation Index (EVI). The VI have been used to monitor plant productivity due to their positive correlation with the fraction of absorbed photosynthetically active radiation (fPAR) and Leaf Area Index (LAI), which are both used to calculate photosynthetic activity (Myneni et al. 1997; Fensholt et al. 2004; Fang et al. 2005). Because of these relationships, MODIS is considered suitable and is commonly used for monitoring spatial and temporal patterns of vegetation including those in semi-arid regions (Colditz et al. 2007; Wistebaar 2008; Sjöström et al. 2011; Davis 2012).

NDVI is calculated as a ratio between the maximum absorption of radiation in the red (R) spectral band and maximum reflection of radiation in the near infrared (NIR) spectral band (Tucker 1979).

$$NDVI = \frac{NIR-R}{NIR+R} \quad \text{----} \quad (1)$$

NDVI is the most commonly used index due to its simplicity and its reduction of certain type of noise such as illumination and atmospheric variations, cloud shadows, and certain topographic effects (Huete et al. 2002). However, NDVI is known to be influenced by variations in the ground and soil layer both in high biomass regions, and in vegetation-sparse, arid areas (Huete et al. 2002; Pettorelli et al. 2005). Various alternative indices have been proposed to address the shortcomings of NDVI, including the Soil Adjusted Vegetation Index (SAVI, Huete 1988) and the Transformed Soil Adjusted Index (TSAVI, Baret et al. 1989). The Enhanced Vegetation Index (EVI) is one of these measurements, and is designed to reduce the atmospheric noise and canopy background variations (Huete et al. 2002), as well as decoupling the influence of the variation in soil brightness (Solano et al. 2010).

The EVI is expressed as:

$$EVI = G\,\frac{NIR-R}{NIR + C1R - C2Blue + L} \text{ ---- } (2)$$

Where L is the canopy background adjustment, and C1, C2 are the coefficients of the aerosol resistance term. Coefficients adopted for MODIS EVI algorithms are: L=1, C1=6, C2=7.5 and G=2.5 (Huete et al. 2002).

In this study, I used MODIS EVI products at 250 m resolution (MOD13Q1; Table 2.1) because they satisfy both moderate spatial resolution and continuous time-series data with moderately high time resolution among the available satellite data. EVI was found to correlate with estimated gross primary productivity at seven different sites in Africa (Sjöström et al. 2011) and has also been used for monitoring plant productivity in the Kalahari (Colditz et al. 2007; Hüttich et al. 2009; Wessels et al. 2011; Udelhoven et al. 2015). Preliminary analysis suggested EVI and NDVI demonstrated a similar pattern of plant productivity in TKR, however, EVI performed better in being able to express transitional changes in productivity, while NDVI tended to emphasise the contrast. Satellite images which encompassed the reserve for the period February 2000 to November 2015 were downloaded from the NASA's Earth Observing System (EOS) clearing house, Reverb (http://reverb.echo.nasa.gov/reverb/).

Table 2.1 Summary of the satellite data used for this study

Sensor and Satellite	Index	Spatial resolution (m)	Temporal resolution	Time range
MODIS, Terra	EVI	250	16 days	February 2000 – November 2015
Landsat 8 OLI	-	30	-	02 April 2014 15 November 2015
MODIS, Terra & Aqua	Burned area monthly	500	1 month	October 2000 –September 2015

Other Satellite Data

To obtain the vegetation map of TKR, the cloud free, geometrically-corrected, multispectral Landsat 8 Operational Land Imager (OLI) data (captured on 02 April 2014, scene ID LC81740792014092LGN00) were used to perform supervised classification. The bands of images covered the entire reserve and were taken near the peak of the growth season in an above-average rainfall year. The data were obtained from NASA's EOS clearing house, Reverb. Another set of recently acquired multispectral Landsat 8 OLI data (captured on 15 November 2015, scene ID LC81740792015319LGN00) were used to understand the relationship between satellite-derived, vegetation indices and plant cover as measured on the ground. The bands of images were cloud-free and taken on a date similar to the field data collection period, and were downloaded from NASA's EOS clearing house, Reverb. The downloaded images were converted from digital number (DN) to top of atmosphere (TOA) radiance and then corrected for the sun angle as pre-processing before the analysis, using Geosud Toa Reflectance QGIS plugin (version 1.0, Ose - Irstea 2015). In addition, the MODIS burned area product (MCD45A1), which denotes monthly fire occurrence at 500 m resolution, was used to examine the effect of fire on plant productivity in TKR. Data for TKR from the beginning of the 2000-01 growth season to the end of the 2014-15 growth season were available from NASA's EOS clearing house, Reverb.

Environmental Data

Daily rainfall data, collected from 30 rain gauges for the period 2001 to 2014 and which were provided by Tswalu Kalahari Reserve, were used in the analysis. In addition, monthly rainfall records from five neighbouring rainfall stations (van Zylsrus, Kathu, Severn, Wildebeesduin, and Upington) were obtained from the South African Weather Service (South African Weather Service 2015). To characterise the environmental conditions of the vegetation types, a 30 m resolution digital elevation model (Shuttle Radar Topography Mission 1 Arc-Second Global) downloaded from the United States geological survey's data portal site, EarthExplorer (http://earthexplorer.usgs.gov/) and detailed GIS layers of soil types in South Africa (CSIR 2012) were used in the analysis.

Field Data Collection

To investigate the relationship between satellite-derived information and field observations, vegetation cover was estimated by line transect surveys in the field at pre-determined sample points. Since previous studies cautioned the use of VI derived from EO data, this study aimed to assess the potential of VI for vegetation studies in the Kalahari. However, it should be noted that this field work was done under extreme drought conditions and vegetation cover and EVI were substantially less than during average rainfall years. The sample points were randomly selected within 150 m distance from the road for Koranna-Langeberg Mountain Bushveld, and 60 m distance from the road for other vegetation types. Locations of these points were set at the centre of the grid on the Landsat OLI images using QGIS (version 2.10 pisa, QGIS Development Team) (Fig. 2.1).

The size of the grid was set at 90 x 90 m, which is equal to nine pixels on the Landsat image, and adjacent to the focal pixel in the centre. Firstly, the homogeneity of vegetation structure and the absence of artificial structures were confirmed at each sampling site. Next, three parallel 30 m line transects along a magnetic north-south bearing were set up in the centre of the focal grid. Plant cover for each growth form (tree, shrub, grass, or forb), bare soil, or rock outcrop was recorded in the grid at one meter interval, and a total of 93 points were assessed per grid. Then, vegetation cover for the focal grid was estimated by calculating the frequency of plant cover per number of points. Five dominant species from the grid were recorded to understand the species composition of the vegetation types. Additionally, the location of degraded areas, such as areas with very little grass cover and bare soil area were recorded. Field data collection was undertaken from 18th - 25th of November 2015.

2.3 Analysis

Classification of Vegetation

The values derived from multispectral bands of the Landsat OLI data (captured on 02 April 2014, scene ID LC81740792014092LGN00) Band B2 – B7 (blue, green, red, near infrared, SWIR1, and SWIR2) were used for supervised classification with a maximum likelihood algorithm. A comprehensive set of photographs taken in May 2015 of the main vegetation units in TKR was used as a training dataset. This was augmented by high resolution satellite images from Google Earth (Google Inc 2015), when referring to the national vegetation map (Mucina & Rutherford 2006) for the vegetation classes. Based on this approach a total of 69 areas with 68 783 pixels of training samples were generated (Table 2.2). The semi-automatic plugin of QGIS (Congedo 2013) was used for pre-processing and classification. The routines of post-processing included filtering the isolated pixels or noise, and smoothing class boundaries. These routines were performed using ArcMap Spatial Analyst extension (version 10.0 ESRI, Redland, USA). The final product which comprised a Landsat-based vegetation map was amalgamated into a single image and used for further analysis.

Table 2.2 Summary of the training sample for the supervised classification which was used to produce a Landsat-based vegetation map for Tswalu Kalahari Reserve. The size of the pixels was 30 x 30 m, which is equivalent to Landsat OLI data.

Vegetation type	Number of areas	Numbers of pixels
Koranna-Langeberg Mountain Bushveld	14	13 701
Gordonia Duneveld	14	38 559
Gordonia Plains Shrubveld	11	9 653
Kathu Bushveld	11	2 565
Olifantshoek Plains Thornveld	19	4 305
Total	69	68 783

Quantifying Phenometrics

The seasonality parameters of the vegetation indices were extracted from time-series MODIS data using the software package TIMESAT (Jönsson & Eklundh 2004). TIMESAT smooths the vegetation indices time-series data by fitting a continuous curve and filtering noise and recognises nine different measurements, such as the beginning of the plant growth season, the end of the plant growth season, and the maximum and minimum value for each pixel (Fig 2.3). These phenometrics were grouped into "phenology metrics" and "productivity metrics" according to their characteristics (Wessels et al. 2011) (see Appendix A, Table A1). TIMESAT has been used in a number of studies to smooth and quantify often noise-corrupted remote sensing data (e.g. Sjöström et al. 2011; Wessels et al. 2011; Davis 2012; Fensholt et al. 2013). The adaptive Savitzky-Golay filter with the window width of four data points was applied to smooth the data. The season per year was set at 1 because vegetation in the Kalahari has one growth season a year. The start and end of the growth seasons were defined as a 20% increase in the seasonal amplitude, measured from the left and right minimum levels to the maximum of the seasonal curve. These values were determined by visually inspecting the fitted curve on the TIMESAT GUI following the software manual (Eklundh & Jönsson 2012), but also by referring to earlier studies from the region (Wessels et al. 2011; Davis 2012).

The means of the 15 year annual metrics were computed for each pixel, as well as the coefficient of variance (CV) for the productivity metrics and standard deviation (SD) for the phenology metrics.

These means of the phenometrics were compared across the vegetation types, and a principal component analysis (PCA) was performed to determine the underlying pattern using PC-ORD Multivariate Analysis of Ecological Data (Version 6. MjM Software). In some years, TIMESAT did not detect phenological parameters due to the low and ambiguous peak of the vegetation indices caused by erratic rainfall. Such values were removed from the calculation of the mean, CV, and SD but were included in the calculation of the small and integrated values as well as the amplitude of the season.

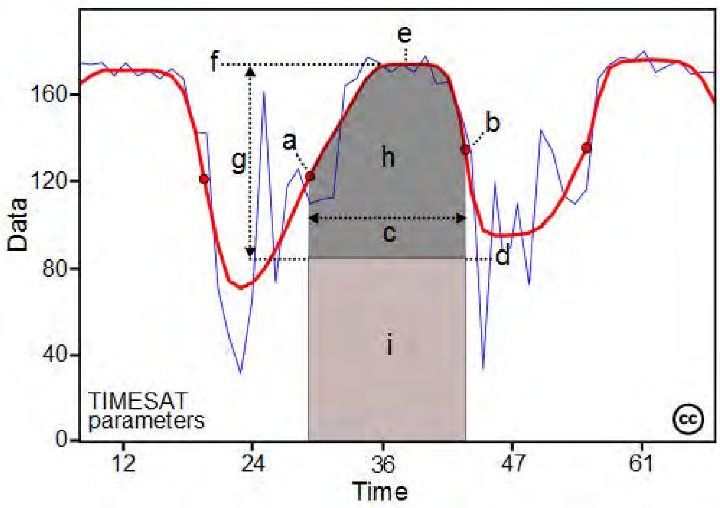

Fig. 2.3 An example of the phenometrics output extracted from satellite data by TIMESAT where (a) beginning of season, (b) end of season, (c) length of season, (d) base value, (e) time of middle of season, (f) maximum value, (g) amplitude, (h) small integrated value, (h+i) large integrated value (after Eklundh & Jönsson 2012). The blue line shows raw values from satellite data, while the red line indicates smoothed values.

Validating Satellite Data and Filed Data

The EVI values derived from Landsat 8 OLI and vegetation cover values estimated from the transects were compared by correlation analysis. EVI values were computed from pre-processed B2 (Blue), B4 (Red), and B5 (NIR) bands of recently-obtained Landsat 8 OLI data following equation (2) above. Correlative relationships with EVI values were explored for 1) total vegetation cover (all growth forms), 2) woody cover (trees and shrubs), and 3) herbaceous cover (grasses and forbs) separately, and vegetation cover was expressed as the ratio of the growth forms recorded from the transects in the focal grid during field work. Spearman’s correlation coefficient between EVI and herbaceous, woody and total vegetation cover was performed for each vegetation type.

Interpolated Rainfall

To understand the geographical variation in rainfall, a spatially continuous rainfall surface was generated by interpolating the rainfall records from 30 stations distributed throughout TKR. Firstly, the original data from rain gauges and weather stations were formatted by removing incomplete and suspect records. Next, total rainfall for the growth season, which starts at the beginning of October and ends at the end of September in the Savanna Biome in South Africa (Wessels et al. 2011), was calculated as the annual rainfall for each rainfall station.

Several algorithms have been proposed to produce an interpolated rainfall surface, including inverse distance weighting (IDW), thin-plate smoothing spline, liner regression, and various types of kriging (Goovaerts 2000; Di Piazza et al. 2011; Ly et al. 2013). However, geostastical interpolation methods such as kriging appear to be preferable when estimating an annual rainfall surface (Ly et al. 2013). Therefore, this study applied ordinary kriging, the simplest form of geostatistical interpolation based on the statistical models involving autocorrelation, to produce rainfall data. A spherical model was selected to fit a semi-variogram, which is the most-commonly used model to interpolate rainfall (Ly et al. 2013), while other parameters were set at default values. In order to match the interpolated annual rainfall surface to the MODIS raster image, the Geostastical Analyst tool in ArcMap (version 10.0 ESRI) was used to perform ordinary kriging for the period from 2001-02 to 2013-14 growth seasons at 250 m spatial resolution.

Relationship between Rainfall and EVI

In semi-arid areas, rainfall strongly affects plant productivity. Thus an understanding of the magnitude of the effect of rainfall is not only important to understand vegetation dynamics, but also to distinguish the effect of rainfall from other drivers (Schwinning et al. 2004; Wessels et al. 2007; Davis 2012; Fensholt et al. 2013).

To evaluate the effect of rainfall on plant productivity, Spearman's correlation coefficient between the annual rainfall derived from the interpolated rainfall surface (explanatory variable) and the small integrated value of EVI quantified by TIMESAT (response variable) was computed for each vegetation type. Earlier studies often used ΣNDVI, calculated from annual sum of NDVI or sum of NDVI during the growth seasons as a proxy for the NPP (Pettorelli et al. 2005; Wessels et al. 2007, 2012). However I used the small integrated value of EVI estimated by TIMESAT. The small integrated value also provides a good estimate of the production of the seasonally-dominant vegetation type (Jönsson & Eklundh 2004), and recent studies have found that the small integrated value of VI estimated by TIMESAT has better agreement with annual primary production in the Sahel (Fensholt et al. 2013; Mbow et al. 2013). Additionally, preliminary analysis showed that the annual small integrated value of EVI exhibited a higher correlation with cumulative rainfall. Different responses to rainfall across vegetation types were tested by ANOVA and post-hoc Tukey's HSD test. Vegetation types were assigned by upscaling the 30 m resolution Landsat-based vegetation map to 250 m grid, which matched precisely to the MODIS data, by allocating the dominant vegetation type in each 250 m grid. All statistical analysis was done using R (version 3.0.1, R Core Team).

Degradation Trends

Rain-use Efficiency (RUE)

Rain-use efficiency (RUE) is one of the analytical techniques used to distinguish anthropogenic degradation from the inter-annual variability of rainfall in arid and semi-arid regions. RUE is expressed as the ratio of net primary productivity against rainfall for a specified period, and a decline in RUE over time is considered to be an indication of degradation (Wessels et al. 2007; Davis 2012; Fensholt et al. 2013). The small integral of EVI estimated by TIMESAT was used to represent annual net primary productivity, and this value was then divided by the corresponding interpolated rainfall surface value to calculate annual RUE. The annual RUE was computed and then regressed over the 2001-2013 growth seasons to investigate long-term trends in degradation.

Residual trends (RESTREND)

Residual trends (RESTREND) were analysed using each growth season (Oct-Sep) as a time step. RESTREND assesses the trend of degradation based on a concept similar to RUE. However, by removing the effect of rainfall from the long-term trend in productivity, this approach can highlight human-induced land degradation. While the detectability of RESTREND has been questioned in arid areas or when the intensity of degradation is weak, this method has been used and has successfully captured degradation patterns at a national scale (Wessels et al. 2007; Wessels et al. 2012).

The regression from 13 growth seasons of times-series EVI and rainfall data was computed following Wessels et al. (2007). First, the regression of the small integrated value of EVI (responsive variable) and cumulative rainfall (explanatory variable) was calculated for the growth seasons for each pixel. Then, trends in the residual, expressed as the difference between observed EVI and predicted EVI by rainfall, were regressed through the growth seasons (Wessels et al. 2007; Wessels et al. 2012). The results were mapped to determine the distribution pattern of degraded areas. Data from the 2006-07 growth season (October 2006 to September 2007), when TKR experienced a severe drought, was excluded from this analysis. This was because when rainfall is too low to detect an active response in plant productivity, small values may cause a bias and disproportionally affect the underlying regression model.

3 Results

3.1 Distribution of the Vegetation Types in Tswalu Kalahari Reserve

Five vegetation types were classified in the Tswalu Kalahari Reserve (TKR) (Table 3.1). The overall spatial patterns of the vegetation types were aligned to Mucina & Rutherford (2006), but the Landsat-based map illustrated the vegetation types in greater spatial detail (Fig. 3.1; see also Appendix B). The Landsat-based vegetation map was derived solely from the Landsat OLI reflectance values measured by the on-board satellite sensors, and did not consider species composition or climate gradients. To identify and compare these Landsat-based vegetation types to those that have already been described by Mucina & Rutherford (2006) will require detailed vegetation surveys including an analysis of species composition. However, that was not within the scope of this study. Field observations recognised a general correspondence between topography, plant community structure and the Landsat-based vegetation types. For example, the relatively mountainous Koranna-Langeberg Mountain Bushveld vegetation was comprised predominantly of a mixture of trees and shrubs, Gordonia Duneveld was dominated by grasses, Gordonia Plains Shrubveld, by dwarf shrubs and Olifantshoek Plains Thornveld by thornveld and thicket vegetation (Fig. 3.2). Field assessments based on these relationships and the distribution of different plant growth forms demonstrated an overall good agreement with the Landsat-based vegetation map. However, disturbed areas such as old artificial water points were often misclassified as Gordonia Plains Shrubland. Likewise, some of the pans in the west of TKR were incorrectly designated as being part of the Koranna-Langeberg Mountain Bushveld. In addition, the boundaries of the vegetation types were not always distinct and were often mixed at the margins, particularly among Gordonia Duneveld, Kathu Bushveld, and Olifantshoek Plains Thornveld.

According to the Landsat-based vegetation map, the Koranna-Langeberg Mountain Bushveld was mostly distributed in the central part of TKR, along the Korannaberg Mountain Range at the altitude of 1160 -1460 m above sea level. Results from field observations showed that in this vegetation type rock outcrops were frequently exposed at the surface, and small trees and shrubs including *Croton gratissimus, Rhus burchellii*, and *Ziziphus mucronata,* and grass species such as *Aristida diffusa* and *Digitaria* sp. grew in the crevices of the rocks. Gordonia Duneveld mainly occurred in the central part of TKR, where the distinctive NNE-SSW aligned dune strips of 0.5 - 1 km intervals have formed as a result of prevailing winds. This vegetation type was dominated by grasses, although species composition varied depending on the topography of the undulating dunes. The crest of the dunes had lower vegetative cover with perennial grasses such as *Eragrostis pallens* and

Stipagrostis uniplumis dominating the area together with the occasional stand of *Terminalia sericea* trees. On the slope of the dunes, perennial grasses such as *E. pallens*, *S. uniplumis,* and *Aristida congesta* ssp. *congesta* usually dominated, and sparse tall shrubs such as *Vachellia haematoxylon* and *Vachellia erioloba,* as well as herbaceous species *Elephantorrhiza elephantine* and *Hermannia tomentosa* were observed. Strips of the dunes typically had higher shrub and tree cover with *Senegalia mellifera, Grewia flava*, and *Rhus tenuinervis* dominating in places. Gordonia Plains Shrubveld was found in the western plains of TKR, and this vegetation was comprised of a mixture of shrubs and grasses. Typically, this vegetation type had 20 - 30% cover of shrubs dominated by *G. flava*, *S. mellifera*, and *Rhigozum trichotomum*. Other common species from this vegetation type included the shrub *Lycium cinereum* and grass species, *Centropodia glauca*. Towards the west of the reserve, the white compact soils distributed in the shallow depressions were dominated by dwarf shrubs including *Monechma incarna* and *R. trichotomum* as well as a sparse cover of tall shrubs such as *S. mellifera* and *G. flava*. Some of the disturbed areas which were present, presumably as a result of past livestock farming practices in the central parts of the TKR and west of the Koranna Mountains, were misclassified as Gordonia Plains Shrubveld, although most of these areas are assumed to belong to Olifantshoek Plains Thornveld. Kathu Bushveld occurred in the central and eastern side of TKR, which was characterised by sparse tall trees including *Boscia albitrunca* and *V. erioloba* and an extensive layer of perennial grass dominated by *S. uniplumis* and *A. congesta* subsp. *congesta*. The Olifantshoek Plains Thornveld was distributed in the eastern part of the TKR and typically formed dense thickets consisting of shrubs such as *S. mellifera, R. trichotomum, G. flava*, and *L. cinereum.*

Table 3.1 Key characteristics of the Landsat-based vegetation types in the Tswalu Kalahari Reserve (see Fig. 3.1). A list of the dominant species is provided for each vegetation type as well as the mean ±standard deviation values for altitude, annual rainfall, soil depth, rock cover and topsoil clay. An explanation of the symbols used to define the major soil types is as follows; Ic: Rock outcrops comprise >80% of land type, Ac: Freely drained, red and yellow, dystrophic/mesotrophic, apedal soils comprise >40% of the land type (red and yellow soils each >10%), Ae: Freely drained, red, eutrophic, apedal soils comprise >40% of the land type (yellow soils comprise <10%), Af: Freely drained, red, eutrophic, apedal soils comprise >40% of the land type (yellow soils comprise <10%); with dunes, Ah: Freely drained, red and yellow, eutrophic, apedal soils comprise >40% of the land type (red and yellow soils each comprise >10%).

Vegetation types	Altitude (m)	Annual rainfall (mm)	Soil				Dominant species
			Major soil type	Depth (mm)	Rock cover (%)	Topsoil clay (%)	
Koranna-Langeberg Mountain Bushveld	1303.6 ± 95.6	347.6 ± 14.4	Ic	555.2 ± 432.0	63.8 ± 37.1	7.8 ± 1.2	*Croton gratissimus, Aristida diffusa , Digitaria* sp., *Grewia flava, Rhus burchellii*
Gordonia Duneveld	1100.1 ± 39.3	312.6 ± 16.1	Af	1176.9 ± 81.8	1.1 ± 2.4	3.2 ± 1.7	*Stipagrostis uniplumis, Eragrostis pallens , Grewia flava, Vachellia erioloba, Vachellia haematoxylon*
Gordonia Plains Shrubveld	1075.6 ± 33.5	304.3 ± 10.5	Af, Ah	1280.4 ± 67.0	1.1 ± 3.6	3.8 ± 1.0	*Centropodia glauca, Senegalia mellifera, Grewia flava, Rhigozum trichotomum, Monechma incanum*
Kathu Bushveld	1157.7 ± 52.4	335.7 ± 18.4	Ae, Af	1215.6 ± 125.5	2.0 ± 8.5	5.3 ± 2.5	*Stipagrostis uniplumis, Aristida congesta* subsp. *congesta, Grewia flava, Senegalia mellifera, Boscia albitrunca*
Olifantshoek Plains Thornveld	1182.4 ± 54.2	342.3 ± 13.7	Ac, Ae	1248.4 ± 174.1	3.7 ± 14.3	6.8 ± 1.6	*Senegalia mellifera, Rhigozum trichotomum, Stipagrostis uniplumis, Grewia flava, Lycium cinereum*

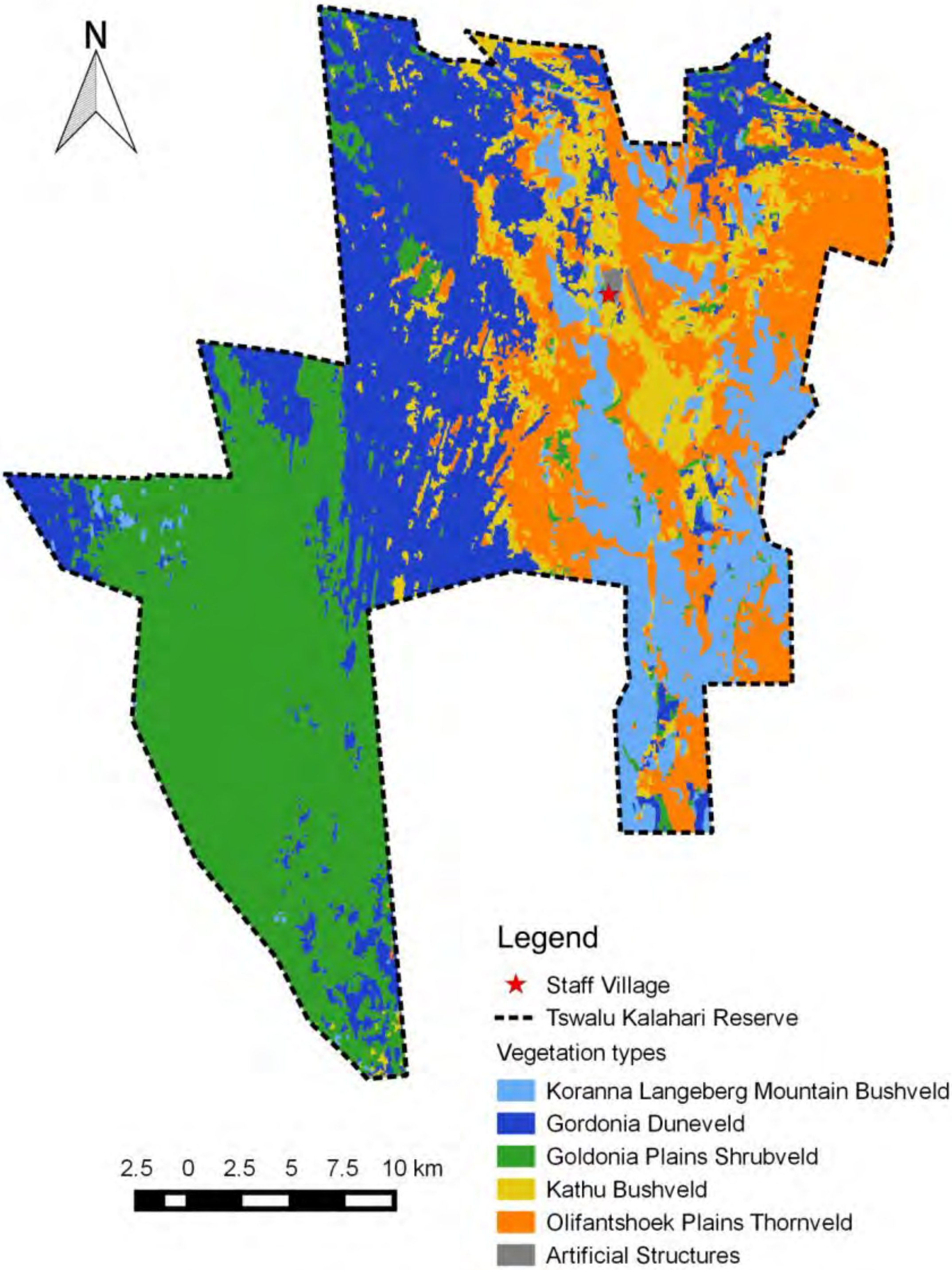

Fig. 3.1 Landsat-based vegetation map for the Tswalu Kalahari Reserve (TKR) classified by using multispectral Landsat 8 Operational Land Imager (OLI). The name of the vegetation types refer to those used by Mucina & Rutherford (2006).

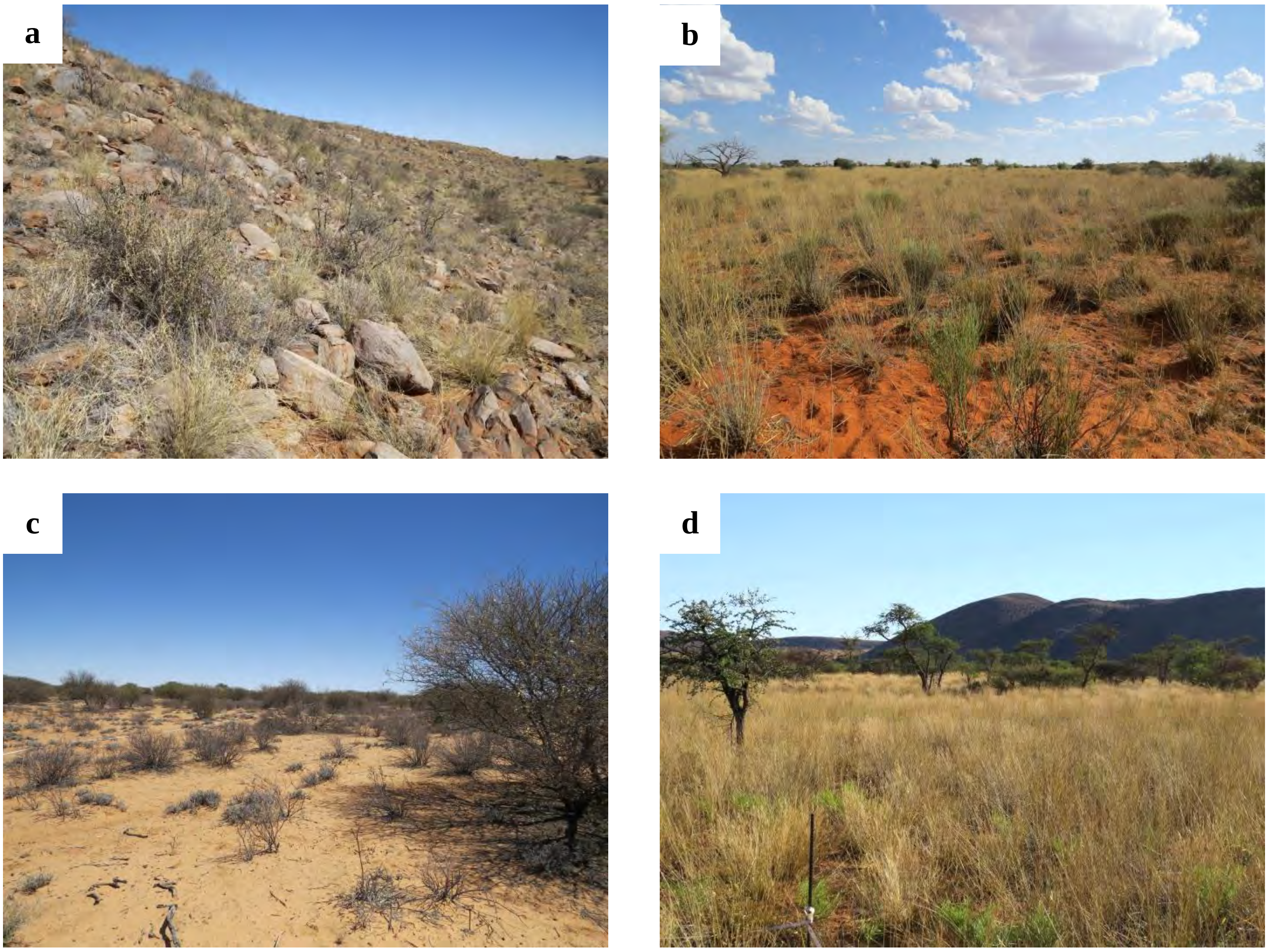

Fig. 3.2 Photographs of the vegetation types in Tswalu Kalahari Reserve, (a) Koranna-Langeberg Mountain Bushveld, (b) Gordonia Duneveld, (c), Gordonia Plains Shrubveld, (d) Kathu Bushveld, and (e) Olifantshoek Plains Thornveld.

3.2 Spatial Pattern of EVI in Tswalu Kalahari Reserve

The overall geographical trend of the mean of the small integral value of EVI, a proxy for annual plant productivity, was higher in the east and lower in the west (Fig. 3.3). There was a significant effect of different vegetation types on all the productivity metrics determined by TIMESAT at the $p < 0.05$ level (Fig 3.4; Appendix A). Post-hoc comparisons indicated that the mean of the small integral value of EVI was significantly different between vegetation types ($p < 0.05$), with Koranna-Langeberg Mountains Bushveld and Olifantshoek Plain Thornveld exhibiting higher values and Gordonia Plains Shrubveld lower values than the other vegetation types. Generally, differences in EVI values between the vegetation types followed a west-east geographical trend.

Differences in the structure of the vegetation were recognised from the spatial pattern of EVI. For example, the parallel patterns of the dunes were clearly depicted, showing lower productivity on the crests and higher productivity values in the inter-dune areas (Fig. 3.3), which corresponded to the field observations of vegetation cover. Similarly, provincial roads running across the eastern part of TKR were visible as a line of low EVI value. Discontinuous differences of the small integrated value of EVI around the boundary of the vegetation types were observed. With significant differences in productivity metrics measured between the vegetation types, it is assumed that physical attributes of the vegetation such as dominant growth forms, species composition, and soil types, influenced the EVI values.

Ordination of the vegetation types by the phenometrics using principal components analysis (PCA) showed a relative similarity of the phenometrics within Olifantshoek Plains Thornveld, Kathu Bushveld and Gordonia Duneveld. In contrast, Koranna-Langeberg Mountains Bushveld and Gordonia Plains Shrubveld were relatively different from other vegetation types (Fig. 3.5). This similarity was generally coincident with the spatial distribution of these vegetation types. Principal component loadings suggested that principal component 1 (PC1) mainly represented the gradient of productivity metrics, and principal component 2 (PC2) mainly indicated the seasonal variation of the productivity metrics represented by base and maximum values (Fig. 3.5).

The fence-line along and within the boundary of TKR was not visible from the distribution of EVI. The degraded sites observed during the field survey, such as those surrounding the water points and the old farm structures were also not highlighted by the EVI mapping (see Appendix C for the degraded sites). However, several patches of low EVI values located south east of TKR corresponded to the inferred location of water points as observed from Google Earth satellite images.

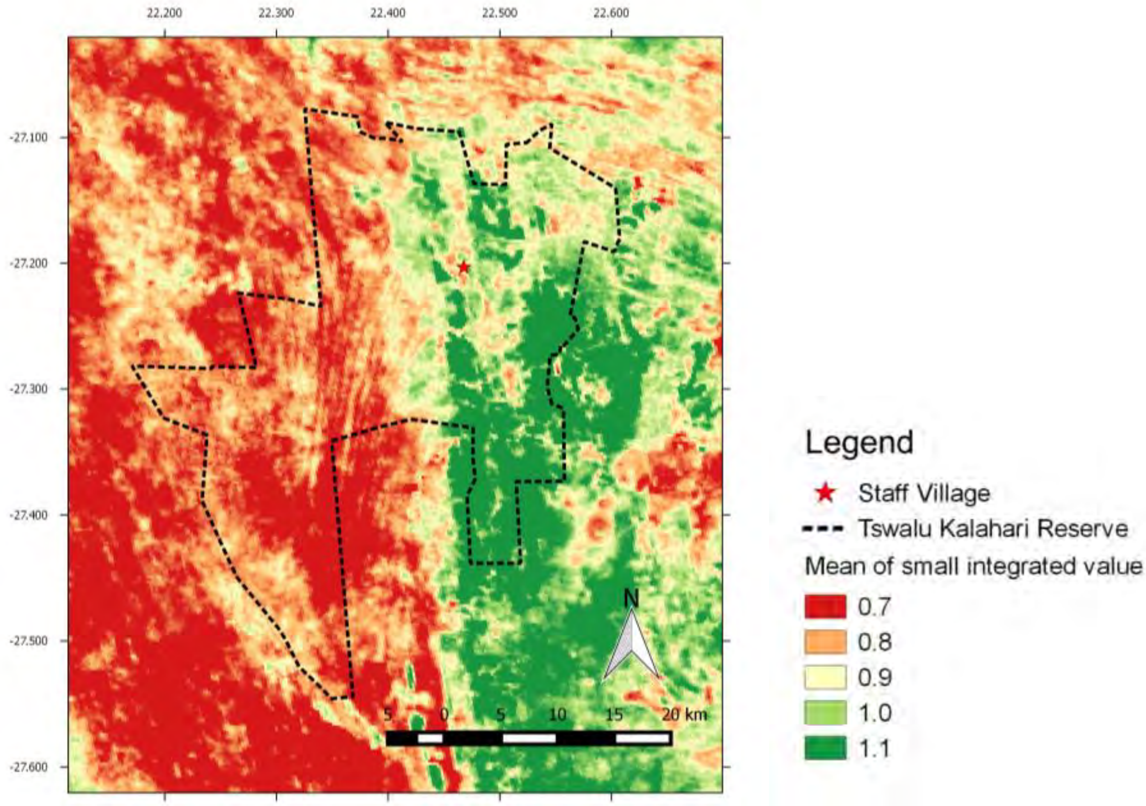

Fig. 3.3 Mean of small integrated value of EVI determined by TIMESAT in Tswalu Kalahari Reserve for the 2000-01 to 2014-15 growth seasons. The small integrated value of EVI is known to correlate with plant productivity and the red colour shows lower productivity, while the green colour shows higher productivity.

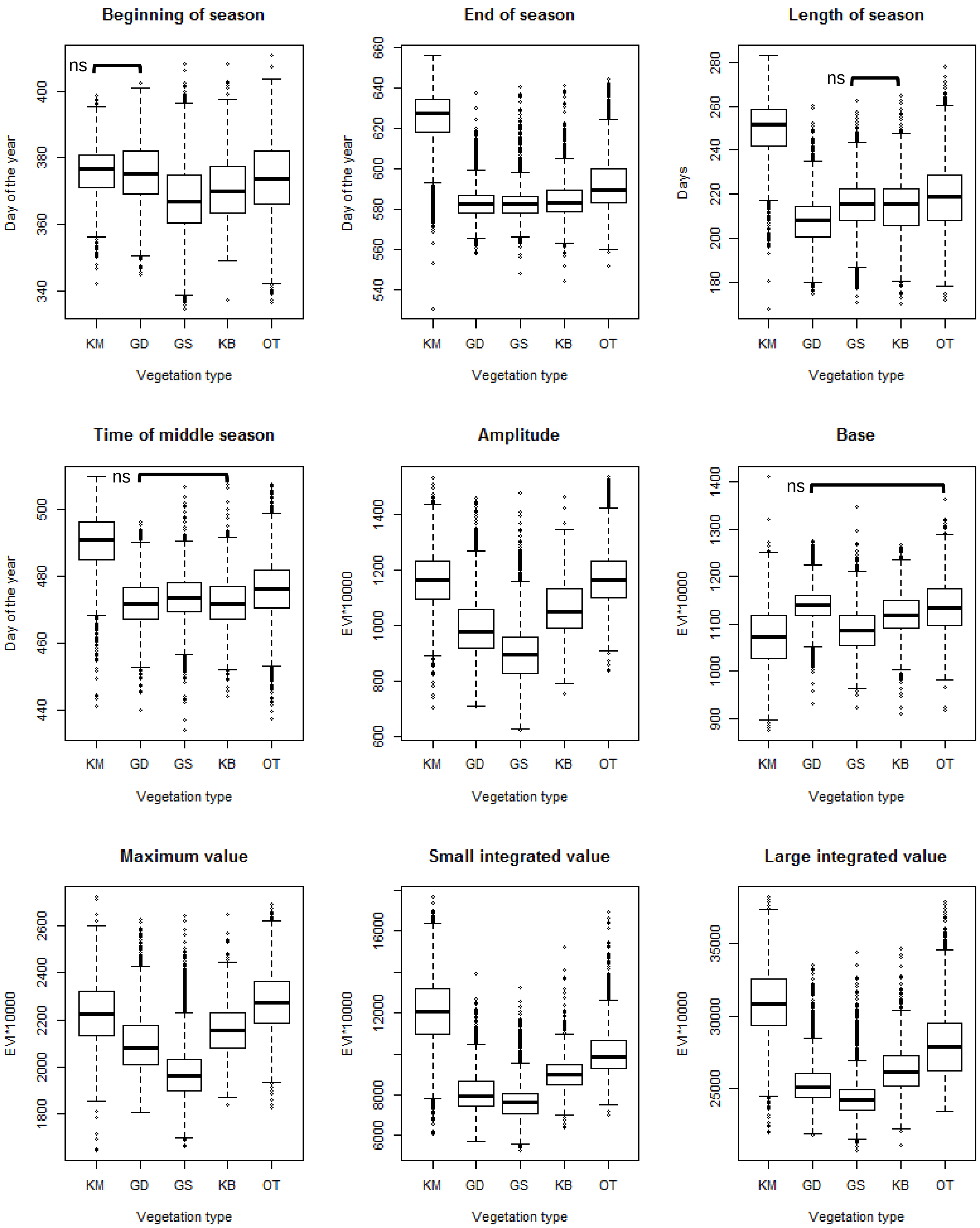

Fig 3.4 Boxplots for the 15 year average for each pixel of phenological and productivity metrics (2000-01 – 2014-15 growth seasons) in the different vegetation types in Tswalu Kalahari Reserve (KM = Koranna-Langeberg Mountain Bushveld, GD = Gordonia Duneveld, GS = Gordonia Plains Shrubveld, KB=Kathu Bushveld, OT = Olifantshoek Plains Thornveld). Post-hoc comparisons using the Tukey HSD detected significant differences (p < 0.05) for all pairs of vegetation types unless noted as ns (not significant).

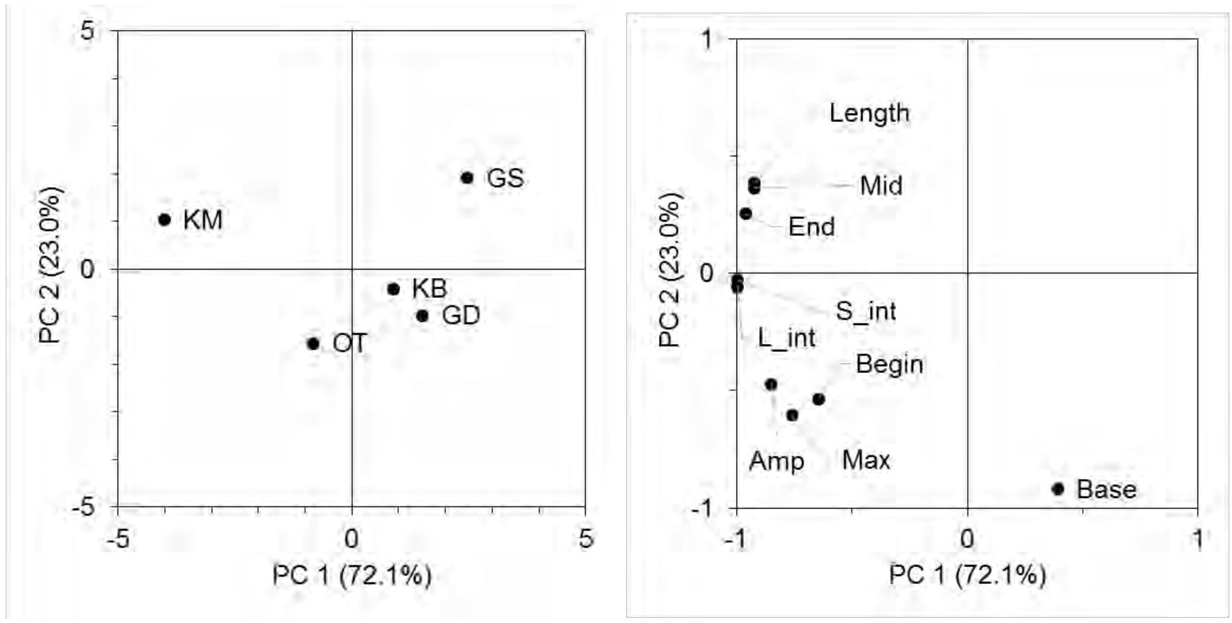

Fig 3.5 The results of a Principle Components Analysis (PCA) for the phenological and productivity metrics for the vegetation types in the Tswalu Kalahari Reserve. The graph on the left shows the principle component loadings while the graph on the right shows the distribution of principle components. KM = Koranna-Langeberg Mountain Bushveld, GD = Gordonia Duneveld, GS = Gordonia Plains Shrubveld, KB = Kathu Bushveld, OT = Olifantshoek Plains Thornveld. Begin = beginning of season, End = end of season, Length = length of season, Mid = time of middle season, Amp = amplitude, Base, Max = maximum value, S_int = small integrated value, L_int = large integrated value.

3.3 Seasonal Trend of EVI

The time-series analysis of EVI values demonstrated a seasonal cycle in plant productivity with high values in the summer months and low values in the winter months (Fig. 3.6). On average, the beginning of the growth season started in the period from December to January, and ended in August to September (Fig. 3.4; Appendix A). ANOVA detected a significant effect of different vegetation types on all the phenological metrics as determined by TIMESAT at the $p < 0.05$ level (Fig 3.4). Post-hoc comparisons suggested that phenological metrics were significantly different among most of the vegetation types with a few exceptions. Korannaberg-Langeberg Mountains Bushveld exhibited a more extended growth season than other vegetation types ($p < 0.01$).

Spatially, the mean value for EVI was more heterogeneous in summer than in winter (Fig. 3.7). In summer, dozens of patches of high EVI values occurred mainly outside TKR, which corresponded to the inferred location of water points as observed in Google Earth satellite images.

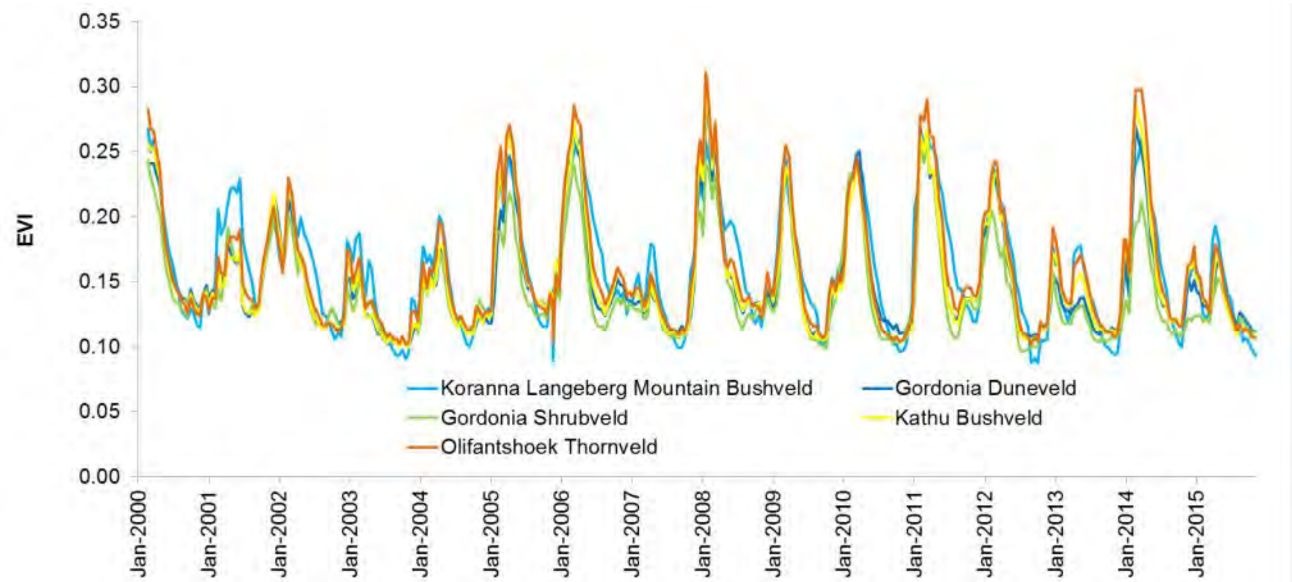

Fig. 3.6 Time series of EVI for the period 2000-2014 for the different vegetation types in Tswalu Kalahari Reserve. Each colour represents a different vegetation type.

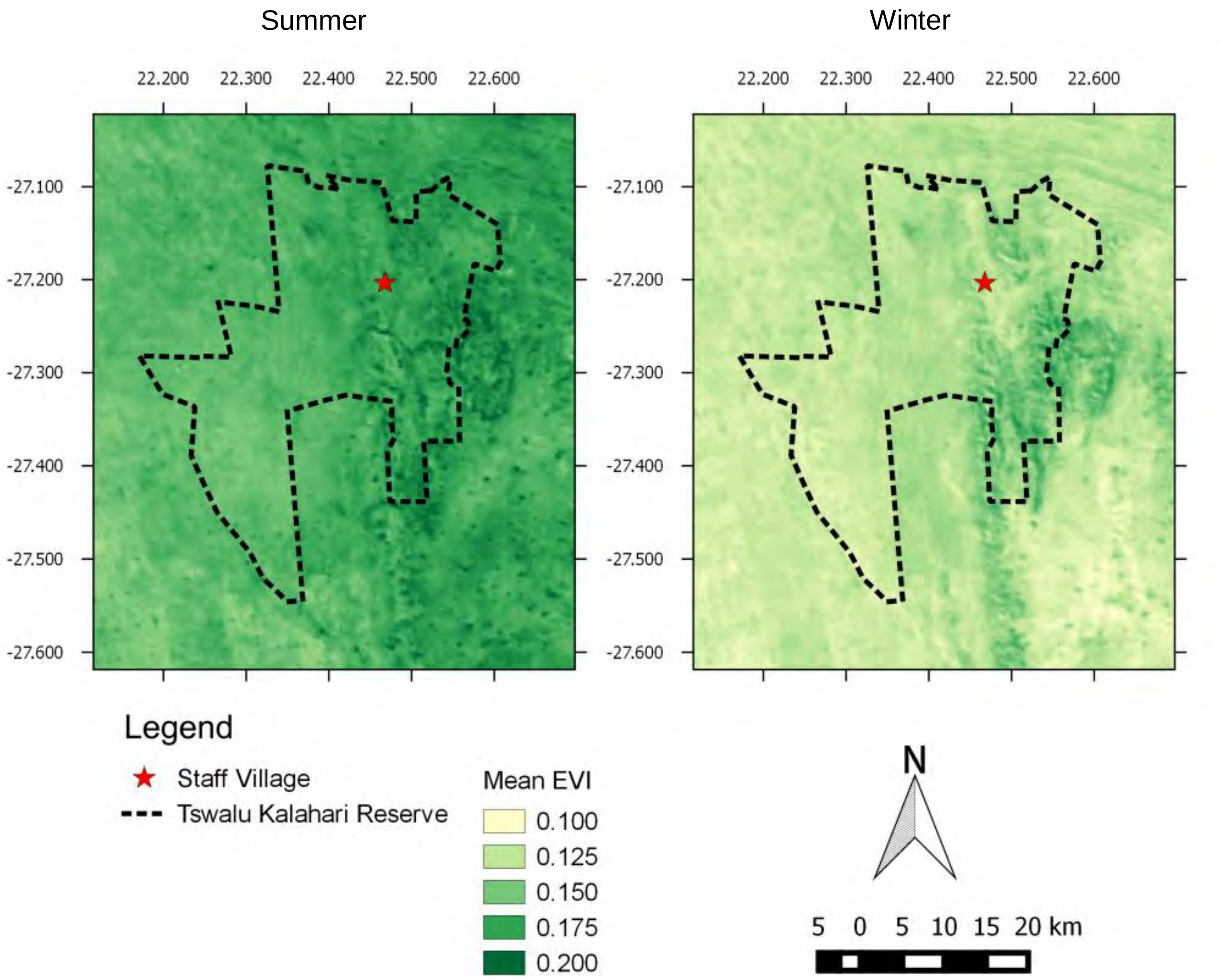

Fig. 3.7 The mean of EVI in the different seasons from 2001 to 2015 in Tswalu Kalahari Reserve. Left map shows the mean EVI of the summer period (1st Jan – 23rd Mar, six images) and right map shows mean of the winter period (27th Jun – 15th Sep, six images)

3.4 Long Term Trend of EVI

The time series of EVI for the past 16 years in TKR illustrated high inter-annual variability in plant productivity (Fig. 3.6). EVI values changed dynamically and low values were evident during the 2000-01, 2002-03, 2003-04, 2006-07, 2012-13 and 2014-15 growth seasons, which corresponded to low annual rainfall (Fig. 3.8; Appendix D). In the 2006-07 growth season, when the annual rainfall was lowest for the study period, TIMEAT failed to quantify the productive metrics for some pixels due to a low and indistinct peak in EVI.

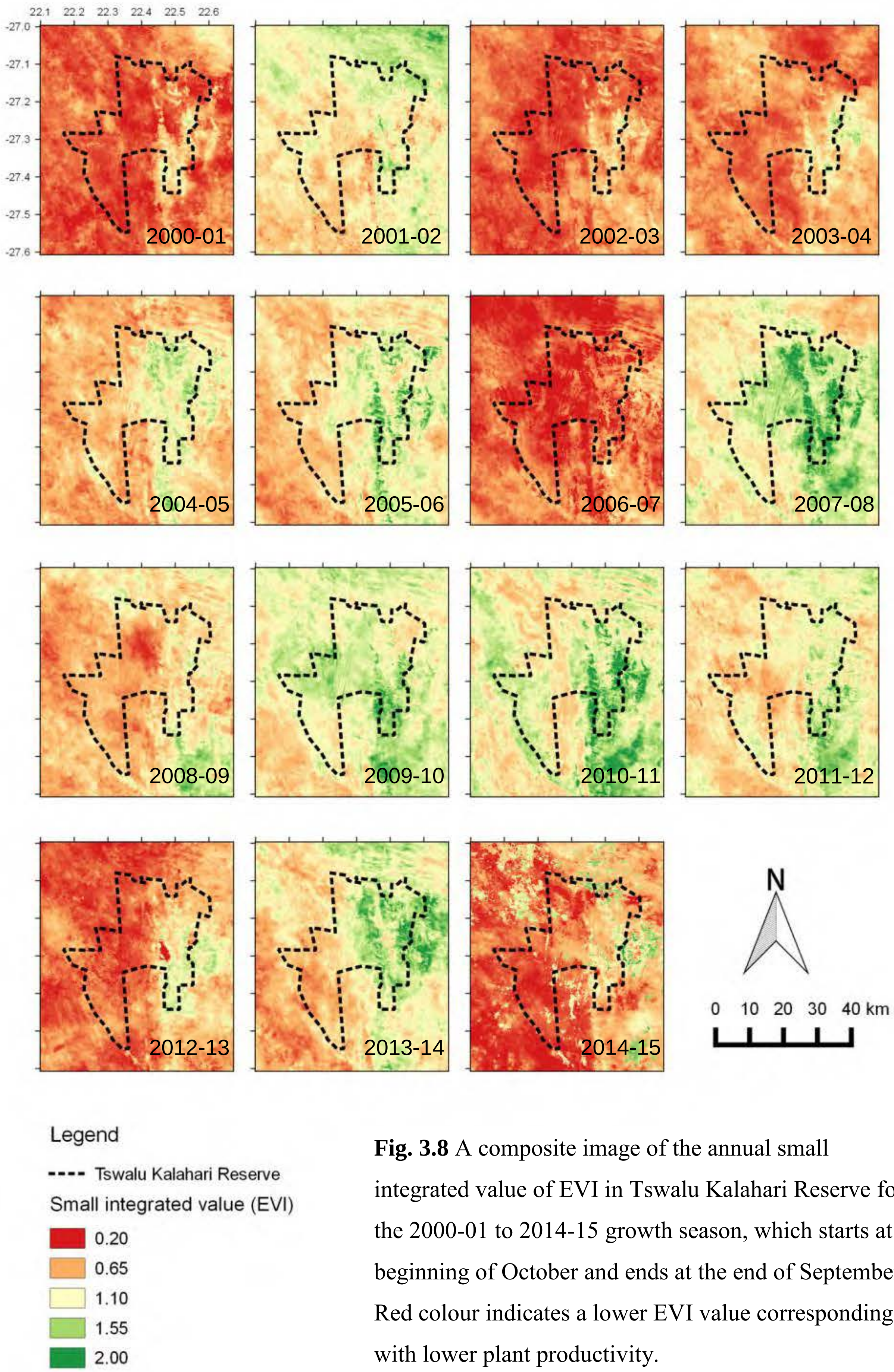

Fig. 3.8 A composite image of the annual small integrated value of EVI in Tswalu Kalahari Reserve for the 2000-01 to 2014-15 growth season, which starts at the beginning of October and ends at the end of September. Red colour indicates a lower EVI value corresponding with lower plant productivity.

3.5 The Relationship between EVI and Vegetation Cover

There was no significant correlation between satellite-derived EVI values and field measured vegetation cover with a few exceptions (Fig. 3.9). The only statistically significant correlation was found for EVI and total vegetation (r = 0. 66, p = 0.04) and herbaceous cover (r = 0.66, p = 0.04) in Kathu Bushveld, and between EVI and woody cover in Gordonia Plains Shrubveld (r = 0.52, p = 0.03). The relationship between EVI and vegetation cover was not consistent across the vegetation types, and data from Koranna-Langeberg Mountain Bushveld demonstrated a different trend from the other four vegetation types.

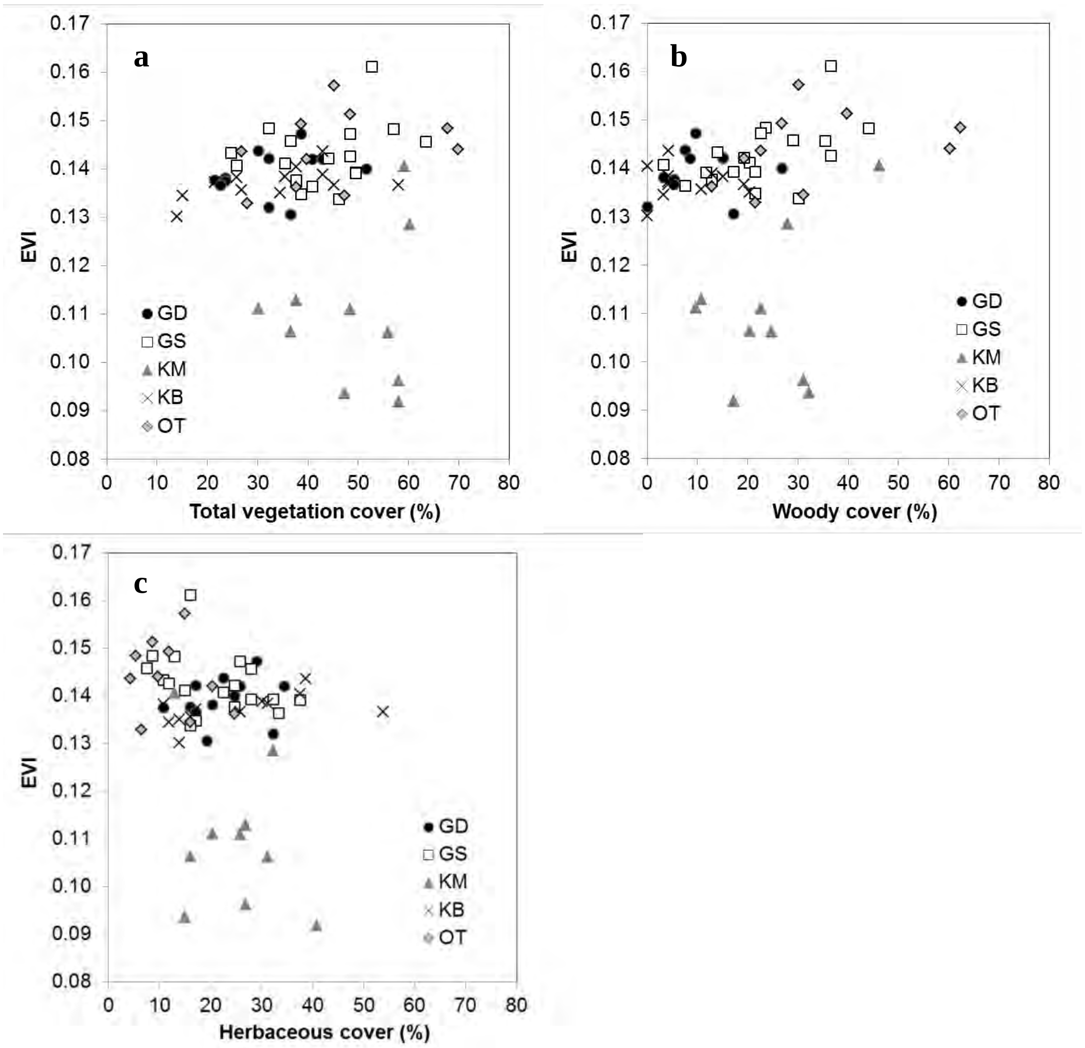

Fig. 3.9 The relationship between enhanced vegetation index (EVI) developed from Landsat 8 OLI data and (a) total vegetation cover, (b) woody cover (trees and shrubs), and (c) herbaceous cover (grass and forbs) estimated by transect survey in Tswalu Kalahari Reserve (KM = Koranna - Langeberg Mountain Bushveld, GD = Gordonia Duneveld, GS = Gordonia Plains Shrubveld, KB=Kathu Bushveld, OT = Olifantshoek Plains Thornveld).

3.6 The Relationship between Plant Productivity and its Potential Drivers

Rainfall

Rainfall has been highly variable over time and space in TKR in the past 15 years (see Appendix D). However, there is a general spatial gradient evident in the data with mean annual rainfall being higher in the east and lower in the west (Fig 3.10). Although the Korannaberg Mountains probably receive higher rainfall than other areas in TKR due to the orographic effects of altitude, this was not confirmed due to the lack of rain gauges on the slopes and peaks of the mountains.

Regression analysis between the small integrated value of EVI and annual rainfall indicated a positive correlation for most of TKR ($p < 0.05$), except in a part of the Roan Sable breeding camp as well as the Kathu Bushveld and Gordonia Duneveld to the east of the Korannaberg Mountains (Fig. 3.11). Different slopes of the regression line among vegetation types also implied that the response of plant productivity to rainfall is specific to each vegetation type (Fig. 3.12).

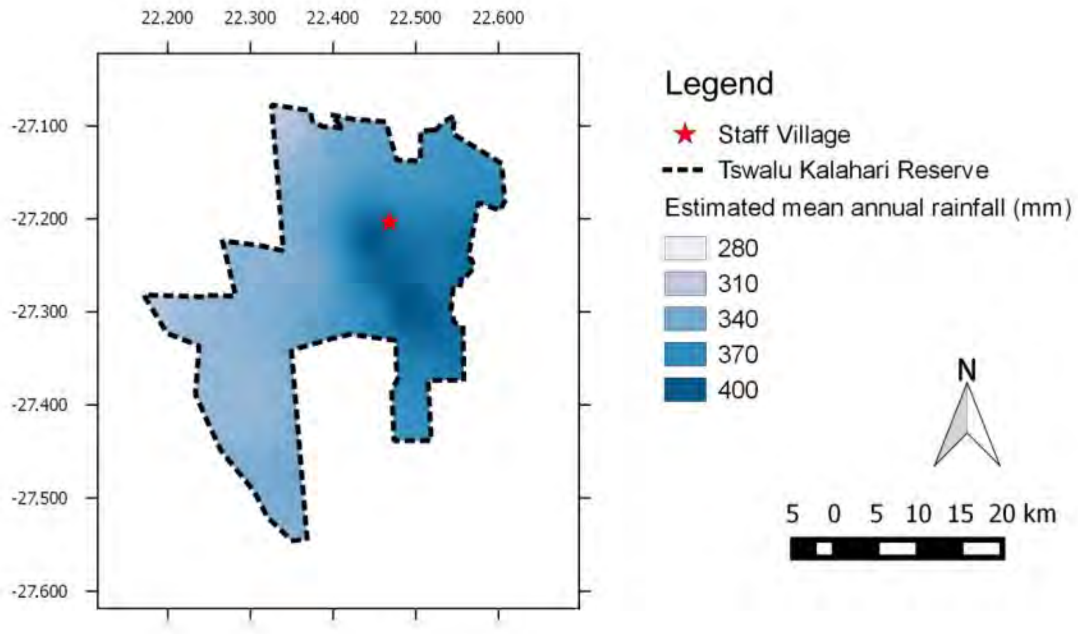

Fig. 3.10 Interpolated mean annual rainfall surfaces by ordinary kriging for the period from 2001-02 to 2013-14 growth seasons in Tswalu Kalahari Reserve.

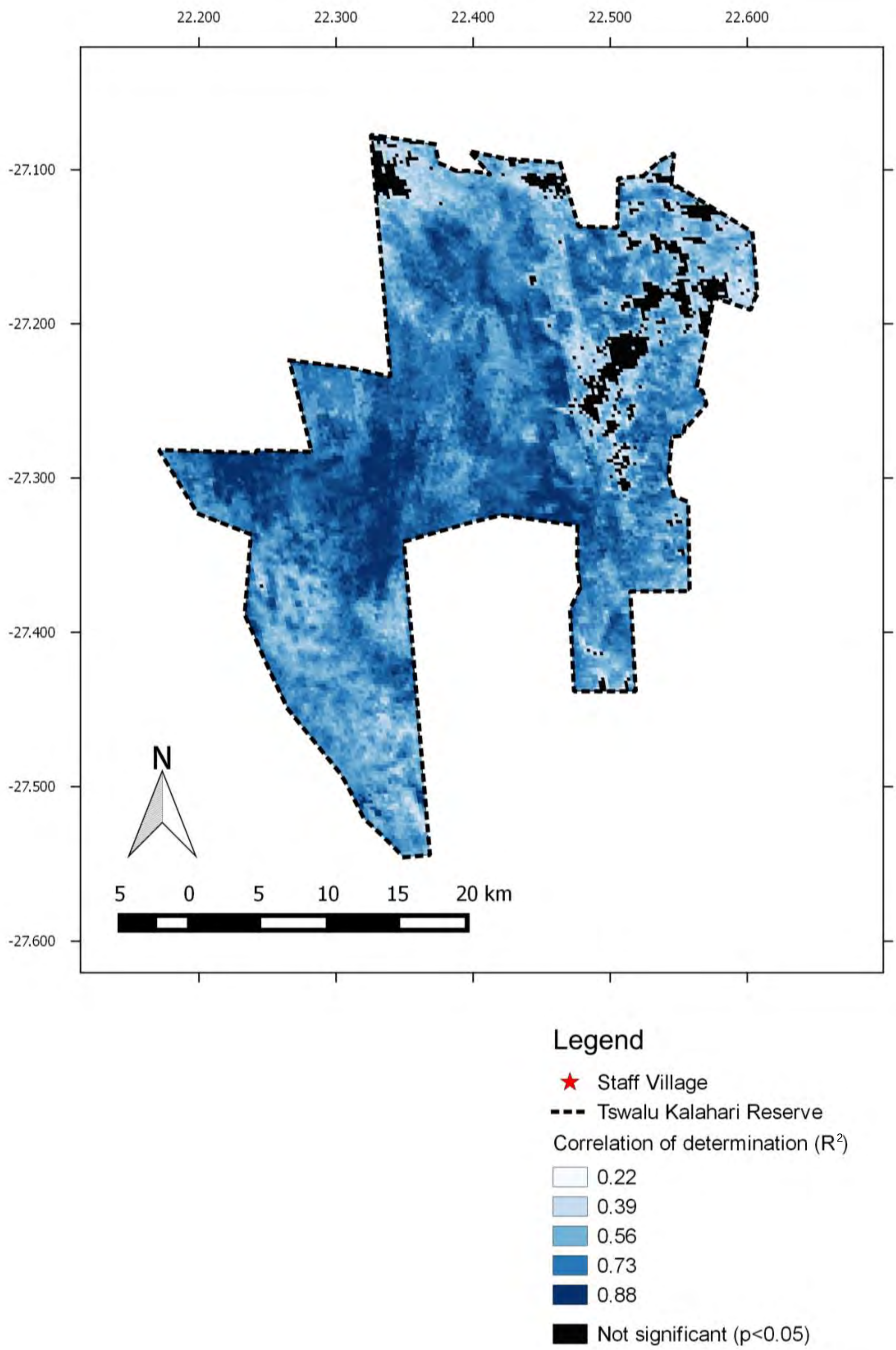

Fig. 3.11 Map of correlation of determination (R^2) of the regression analysis for the annual rainfall for the growth seasons (explanatory variable) and small integrated value of EVI (responsive variable) between 2001-02 and 2013-14 growth seasons, excluding the drought season of 2006-07.

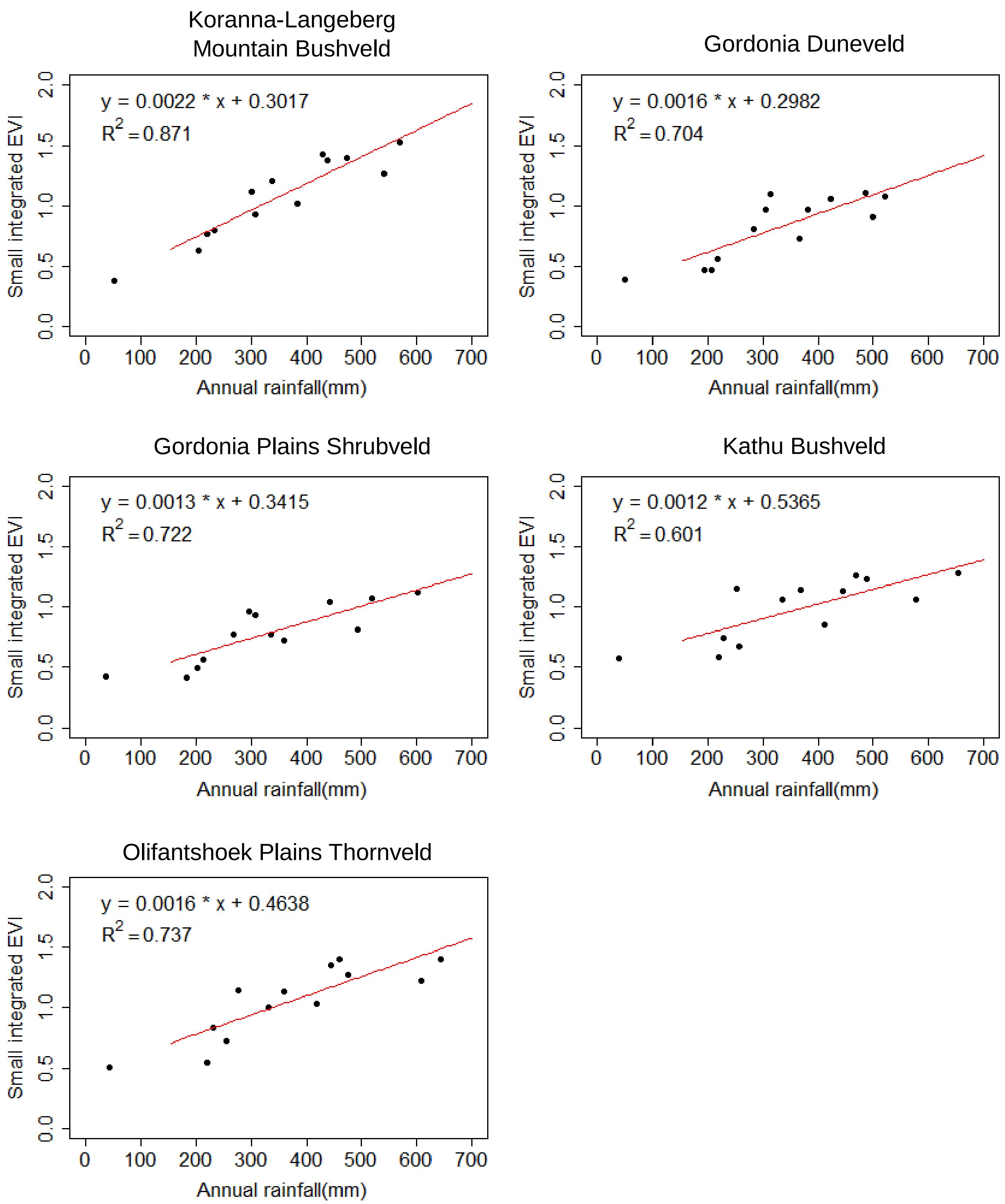

Fig. 3.12 The regression analysis between the average of interpolated annual rainfall surface and the average of small integrated value of EVI for each vegetation type from the 2001-02 to 2013-14 growth seasons in Tswalu Kalahari Reserve. The isolated points in the bottom left corner of the graphs are derived from the poor 2006-07 growth season data. The red line shows the regression relationship between annual rainfall (mm) and Small integrated EVI excluding the data from the 2006-07 growth season.

Fire

Three fire events were evident in the satellite data over the past 16 years in TKR. All of the recorded fires were located in the Korannaberg Mountains in the south eastern corner of the reserve. Consequently, most of the reserve has not burned during the study period (Fig. 3.13). The impact of fire on plant productivity was captured by the small integrated value of EVI, although the response was case-specific. For example, the area south of the staff village which burned in 2012 had a low small integrated value of EVI in 2012, but the area which was burned in 2011 had a more muted response (Fig 3.8). Conversely, the area which burned outside TKR in 2010 showed an increase in the small integrated value in the same season. This result may have been caused by post-fire recovery processes. From these observations, it is assumed that the intensity and date of the fire influences several key characteristics of plant productivity in the growth season immediately after the fire.

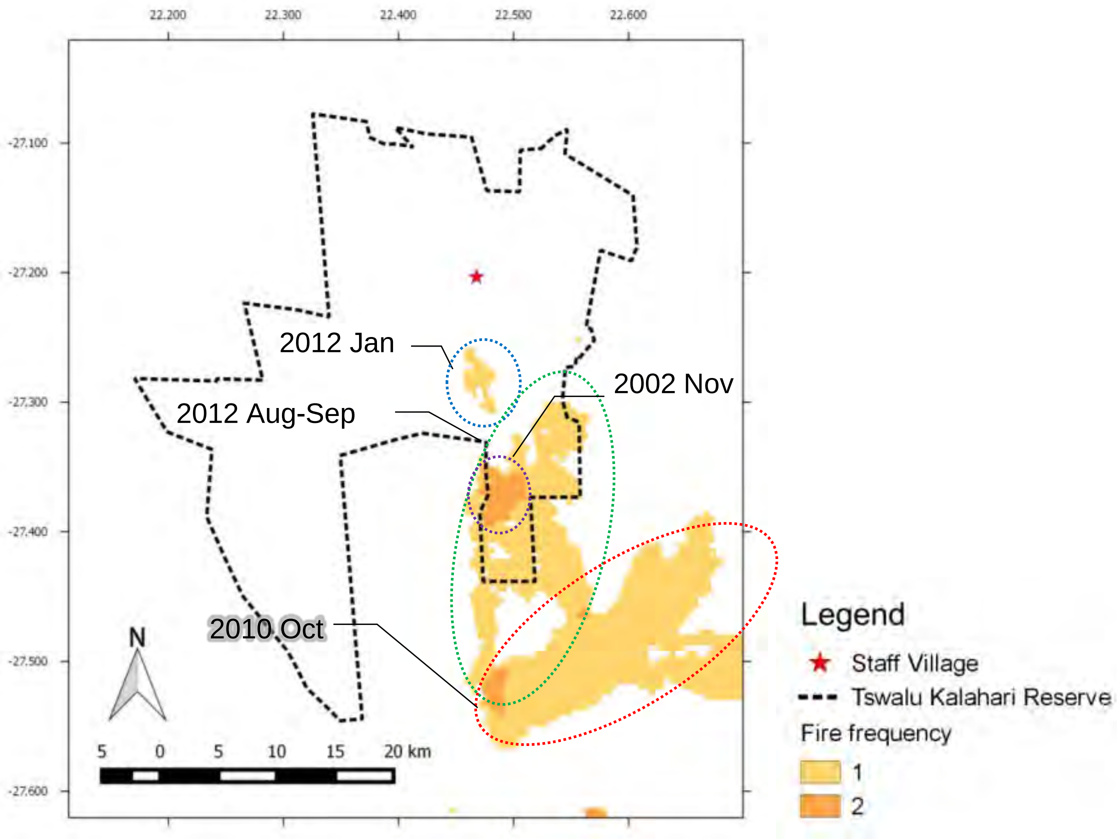

Fig. 3.13 The frequency of fire from 2000-01 to 2014-15 growth seasons delivered from MODIS burned area products (MCD45A1) in Tswalu Kalahari Reserve, indicating that the burned areas in the past 15 years were confined to the mountains in the south eastern corner of the reserve. The numbers on the map indicate the year and month in which the fires occurred.

3.7 Degradation Mapping

Rain Use Efficiency (RUE)

The spatial pattern of mean rain-use efficiency (RUE) was generally highest in Koranna-Langeberg Mountain Bushveld and lowest in Gordonia Duneveld. However, the mean of the 13 year data was strongly influenced by the 2006-07 growth season data, when rainfall was extremely low and RUE was extremely variable (see Appendix E). When the effect of the 2006-07 growth season was removed, mean RUE was still highest in Koranna-Langeberg Mountain Bushveld and lower in other vegetation types (Fig. 3.14a). This spatial pattern was consistent with the mean of the small integrated value of EVI (Fig. 3.3). The lowest mean RUE was observed at the pans and water points in the western part of TKR, but not all the degraded areas observed during the field survey were identified as locations with the lowest RUE values.

The trend in RUE, expressed as the coefficient of regression over time, was not statistically significant for most of the reserve ($p < 0.05$) (Fig. 3.14b). A significant decline in the trend of RUE was observed in several locations in Gordonia Duneveld and Gordonia Plains Shrubveld, while an increasing trend was observed in some pixels in the eastern part of TKR. The general spatial pattern of the trend in RUE was for an increase in RUE in the east, and a decrease in the west. Although the trend was not significant, the burned area in 2012 in the Korannaberg Mountains was clearly depicted as having a declining trend.

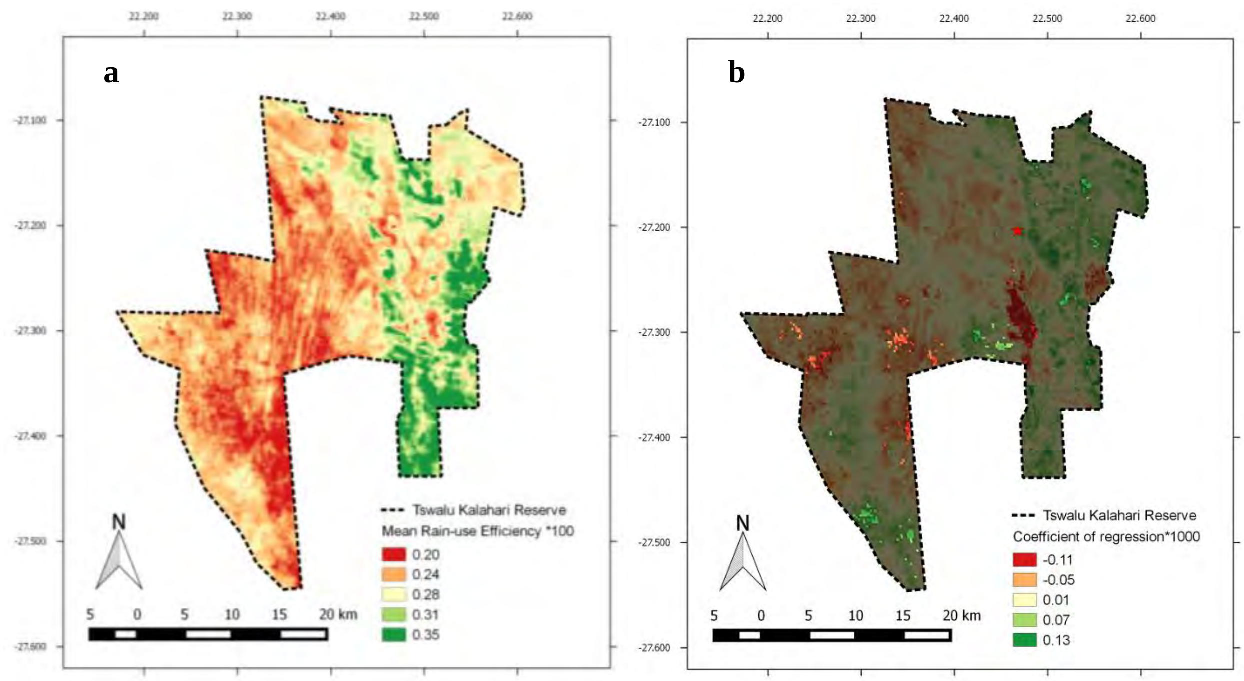

Fig. 3.14 Results of Rain-use efficiency (RUE) analysis showing (a) mean of RUE and (b) slope of the regression of RUE in Tswalu Kalahari Reserve (TKR) for the 2001-02 to 2013-14 growth season, excluding the 2006-07 growth season when TKR experienced a severe drought. The slope of the regression was computed by regressing RUE values for each growth season (responsive variable) against the growth seasons counted from 2001-02 (explanatory variable). Shadowed pixels indicate the areas in which no significant trend was detected.

Residual Trend Analysis

The trend in plant productivity computed by the residual trend analysis (RESTREND) detected a significant positive trend in plant productivity in the east and south west of TKR, while a negative trend was detected in some locations in the west (Fig.3.15). The standardised RESTREND values from these areas demonstrated a relatively consistent and directional change over time (Fig. 3.16). This suggested that the observed change was initiated before the 2000-01 growth season and that the driver of change has remained the same. Most of the area which showed an increasing trend overlapped with shrub-dominated vegetation, especially the Olifantshoek Plains Thornveld in the east and Gordonia Plains Shrubveld in the southwest.

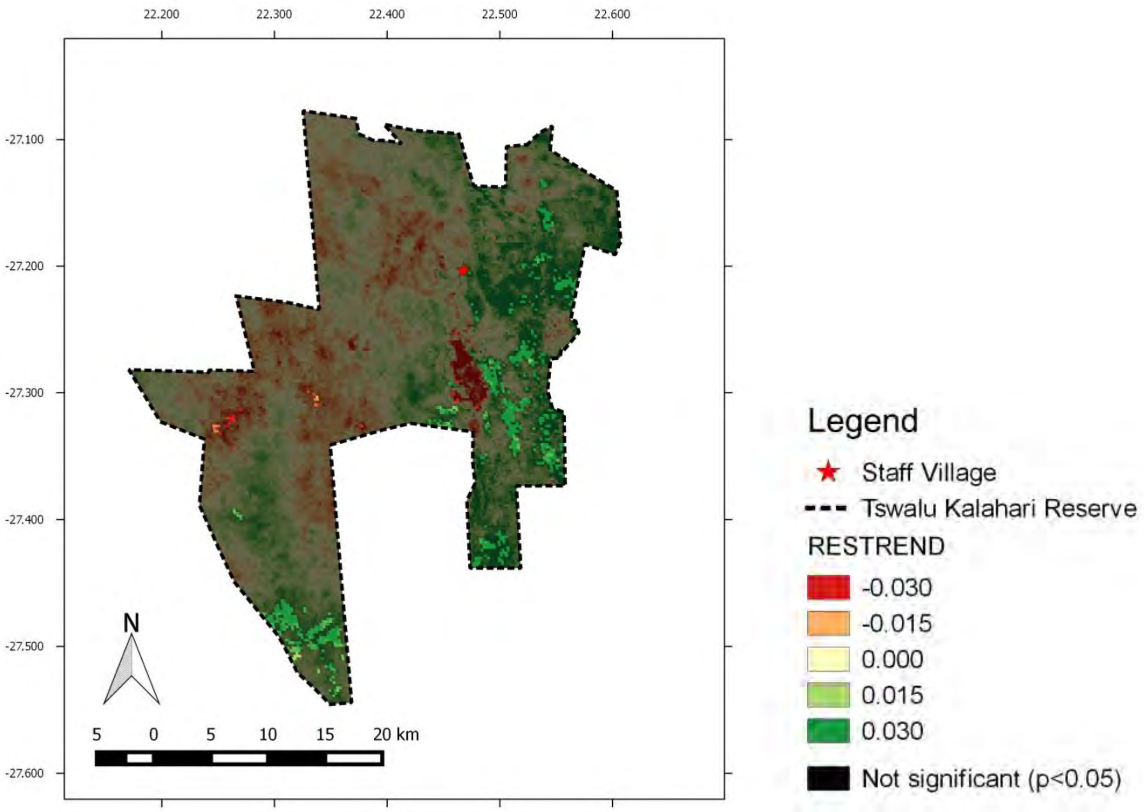

Fig. 3.15 Map of the slope of the residual-year regression analysis of RESTREND. The areas where a significant trend was not found as displayed in shadow. RESTREND analysis showed a significant positive long-term trend in vegetation productivity in the eastern and south western part of Tswalu Kalahari Reserve.

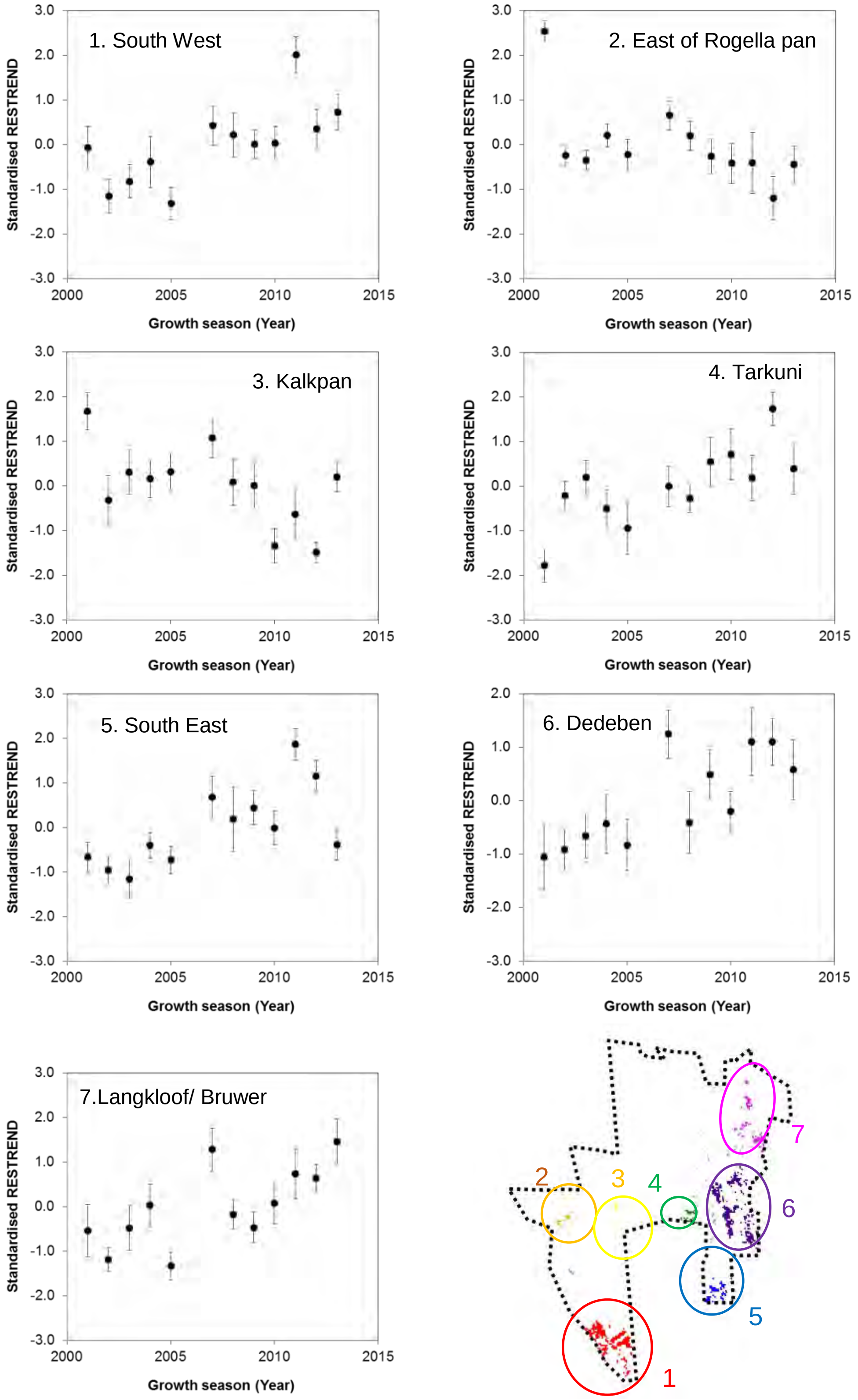

Fig. 3.16 Examples of significant trends in standardised RESTREND values over time from several areas with significant decreasing trends (graph 2 and 3) or increasing trends (graph 1 and 4-7) in Tswalu Kalahari Reserve. Values are shown as mean ± standard deviation in each area. The small map below indicates the areas of data in each graph.

4 Discussion

4.1 Patterns of Plant Productivity in Tswalu Kalahari Reserve

Spatial Patterns

Spatially, the mean small integrated value of EVI increased along a gradient from west to east which coincided with an increasing trend in rainfall. The same geographical trend was recognised in the relative similarity of the productive metrics among the vegetation types. Supported by the general correlative relationship between rainfall and EVI values, the results therefore highlighted the major influence of rainfall in determining vegetation productivity and confirmed the importance of rainfall identified by earlier vegetation studies carried out elsewhere in the Kalahari (van Rooyen et al. 1990; van Rooyen & van Rooyen 1998; Masunga et al. 2013; Mishra et al. 2015a).

The spatial distribution of EVI values also suggested that vegetation type had an influence on vegetation productivity. Each vegetation type was comprised of species with a unique combination of plant structural and functional traits. The Landsat-based vegetation map showed a general trend for increasing and thickening woody cover from the west towards the east. For example, Gordonia Plains in the west was a mixture of grasses and dwarf shrubs, and Gordonia Duneveld in the central and western parts of TKR was predominantly a grassland with shrubs occurring in the depression of the dunes. Kathu Bushveld was open and had more woody cover with sparse tall trees and shrubs, while Olifantshoek Plains Thornveld in the east was mostly thicket vegetation with high woody cover. Mishra et al. (2015b) found woodland areas demonstrate higher VI and the values decreased as the woody cover density decreased (e.g. to an open shrubland or grassland) in the central Kalahari. Therefore, the spatial pattern of vegetation productivity was likely to be related to differences in species traits. Additionally, spatial variation in vegetation types was partly a reflection of the characteristics of different types of soil, which would indirectly also have influenced EVI values. Plants do not respond directly to precipitation, but to soil moisture through variations in infiltration rates, soil depth, and water retention (Jolly & Running 2004; Reynolds et al. 2004). Bare soil associated with different vegetation types could also affect EVI values directly by influencing the level of background noise (Palmer & van Rooyen 1998; Kong et al. 2015). Consequently, it was assumed that changes across vegetation types were likely to be a combination of both the difference in plant functional types and differences in soil types.

Large areas of bare ground around artificial water points illustrated the effects of higher densities of ungulates on vegetation, but EVI mapping did a poor job of identifying these degraded areas. It has previously been reported that degraded areas cannot always be measured by the level of annual vegetation productivity in the Kalahari (van Rooyen 2000). This is because EVI values in degraded areas are as influenced by rainfall as the surroundings. Presumably, annual grasses and herbaceous species such as *Schmidtia kalahariensis* which can emerge quickly in degraded areas after rain, contribute to an increase in EVI values, thereby reducing the difference between degraded and non-degraded areas (van Rooyen et al. 1984; van Rooyen 2000).

Temporal Patterns

Vegetation productivity as represented by time-series EVI values demonstrated strong temporal variation, probably reflecting high seasonal change in vegetation cover (i.e. annual grasses, defoliation) in the Kalahari (van Rooyen et al. 1984). Typically, EVI values increased in the late spring to summer, decreased in the late autumn, and then remained low during the winter. This cycle matched the findings of previous studies used EO data (Jolly & Running 2004; Hüttich et al. 2009; Wessels et al. 2011; Mishra et al. 2015a), as well as field observations in the Kalahari (Sekhwela & Yates 2007), and confirmed the reliability of EVI as a proxy for seasonal vegetation productivity cycles. Annual vegetation productivity characterised by the small integrated value of EVI had a dynamic response to annual rainfall and confirmed the major effect of rainfall in determining vegetation productivity in the Kalahari (van Rooyen & van Rooyen 1998; Masunga et al. 2013; Mishra et al. 2015a).

Seasonal climatic fluctuations and plant structural and functional traits are likely to influence the phenological profile of the vegetation indices in the Kalahari (Mishra et al. 2015a). Among the vegetation types, the start of the growth season varied between years to a greater degree in Gordonia Duneveld (which is comprised predominantly of grass species) and Gordonia Plain Shrublands, while other vegetation types were less variable. In the dry savanna, grasses are known to be highly responsive to rainfall events, while low shrubs generally have limited access to water in the vadose zone, and many of the taller shrubs such as *Senagalia* spp. and *Vachellia* spp. have deep roots that enable them to access more stable underground water sources (Jolly & Running 2004; Sekhwela & Yates 2007). As a result, the phenological responses in woody species are relatively muted in comparison to grass species which response rapidly to water availability (van Rooyen et al. 1984; Scanlon et al. 2002; Archibald & Scholes 2007). In general, the expected response to rainfall from species with these different functional traits matched the spatial and temporal variability in ‘greening up’ at the start of the growth season.

In contrast, the end of the growth season was more variable spatially, rather than inter-annually (Appendix A, Fig. A1). Spatial differences were likely to be due to differences in the characteristics of different plant species in each of the vegetation types, as well as underlying soils. For example, Koranna-Langeberg Mountain Bushveld has an extended growth season compared to other vegetation types (Fig. 3.4), presumably because one of the dominant species, *Croton gratissimus,* retains its mature leaves until the start of the dry season (Childes 1988). Furthermore, evergreen trees such as *C. gratissimus*, generally have higher photosynthesis rates during the winter months in comparison to deciduous trees (van Rooyen et al. 1986). Although not explicitly explored in this study, moisture retention within the rockier slopes on which Koranna-Langeberg Mountain Bushveld occurs might be an additional factor which allows this vegetation type to extend its photosynthetic activity deeper into the dry winter months.

Low inter-annual variability as seen in low standard deviation values for end of the season (Appendix A, Fig. A1), suggests that factors which are more temporally predictable than rainfall, such as day light length or low temperature thresholds could contribute to determining the end of the growth season. However, further analysis is required using higher temporal resolution environmental data in combination with frequent field observations in order to better understand what switches off growth within the TKR.

4.2 Drivers of Plant Productivity

Rainfall

Results confirmed rainfall as a principal driver of vegetation dynamics in this arid region of the Kalahari (van Rooyen et al. 1984; Jolly & Running 2004; Reynolds et al. 2004; Wessels et al. 2007; Mishra et al. 2015a). This is represented as a strong linear relationship between rainfall and EVI which suggests that animal carrying capacity may also fluctuate depending on the amount of rainfall. This poses a potentially growing risk to wildlife and wildlife management under future climate change, as the Kalahari region is expected to experience some of the greatest temperature increases in southern Africa, with concomitant reductions in moisture availability due to reduced rainfall and evaporative loss (Shongwe et al. 2009; Collins et al. 2013; Dai 2013). However, this regression relationship may oversimplify more complex interactions (Wessels et al. 2007). Plants usually respond, not to rainfall but to soil moisture, which is controlled by the water retention capacity of the soil, by run-off, and topography. The size, seasonality, and interval of rainfall events may also affect plant productivity in the drylands (Reynolds et al. 2004; Wessels et al. 2007).

For areas where there was a weak or poor correlation between the rainfall and EVI the influence of factors other than rainfall appears to be important (Fig. 3.11). For example, a significant correlation was not found in the Roan Sable breeding camp in the north-western corner of TKR, probably due to the higher density of animals and possibly uneven intensity of grazing pressure. Additionally, parts of the area which experienced a fire in 2012 did not demonstrate a significant correlation between rainfall and EVI, which might reflect the relatively early stages of post-fire vegetation recovery. Parts of north eastern TKR also exhibited a poor correlation between rainfall and EVI although explanations for this were not immediately evident. Additional field work is required to assess the potential causes that could have influenced the annual rainfall – EVI relationship.

Fire

The effect of fire on vegetation productivity was considered to be of short duration or localised in nature in TKR. According to the EO data, the occurrences of fires were isolated and confined to the south-east of the reserve and as such, most of TKR has not experienced fire in the past 16 years. The spatial pattern of fire occurrence followed a west to east gradient of increasing rainfall, which implies there is probably a link between fire frequency and rainfall. This is because higher rainfall can stimulate greater plant growth and in so doing accumulate greater fuel loads (Thomas & Paul 1991). The responses of plant productivity to fires varied depending on the area and vegetation type but in general, the effect of fire appeared to last for 2 - 3years. However, the low frequency of fires in the past 16 years suggests that the research period may not have been long enough to fully evaluate the impact of fire on vegetation in the reserve.

Herbivory

Between 2005-2014 the number of herbivores within the major part of TKR increased constantly while in the predator camp in the north and eastern part of TKR herbivore density remained stable (D. Smith, personal communication). Results suggested both a degradation effect from heavy grazing, as well as little to no impact in areas of higher rainfall and/or predator presence. For example, herbivore-driven degradation was evident in the Roan Sable breeding camp due to high stocking rates, artificial water points and the provision of supplemental feed. A decline in plant productivity was suspected in a few other locations in TKR, such as in parts of the Gordonia Plains Shrubveld and Gordonia Duneveld in the western part of TKR. This was possibly due to grazing preference in these areas and proximity to artificial water points. In the above examples the degradation trend might be underestimated due to a limitation in the ability of the RESTREND analysis to detect degraded areas (Wessels et al. 2012). In other areas the increased productivity of woody shrubs (as evidenced from the RESTREND analysis), suggested that browsing species such as Kudu and Black Rhinoceros were not able to suppress the expansion of woody species, resulting in bush encroachment.

The observable effect of land use change from livestock farms to a game reserve was not found in this study. Field observations confirmed the presence of piosphere effects around the artificial water points and the old farming structures. But the results did not indicate any trend in vegetation productivity over the study period, and the past satellite images suggested that the degradation around the artificial water points started at least as early as the 1980s, 20 years before TKR was established (see Appendix F). In some early images, the clear differences in vegetation cover evident across fence-lines disappeared in later images as fences were removed and grazing pressure distributed more evenly across the landscape.

4.3 Patterns of Degradation and Long-term Trends

Results of the RESTREND and RUE analysis suggested ongoing bush encroachment and an increase in woody shrub cover especially in the eastern and southwestern parts of TKR, which is likely to have started before this study. The shift in climatic seasonality, in particular the timing of rainfall, could affect the results of the RESTREND analysis by altering growth season (Davis 2012), but the length of the growth season quantified by TIMEAT did not demonstrate a significant trend during the study period for all pixels ($p < 0.05$). Fire, on the other hand, might have had a local effect on the slope of the RESTREND analysis in the south-eastern part of TKR. The area showed relatively high RESTREND values during the 2012-13 growth seasons following a fire at the end of the 2011-12 growth season, which suggested that there was some influence from post fire recovery.

However, this does not account for the broader pattern of bush encroachment evident in the eastern parts of TKR. Earlier studies have noted that bush encroachment can have multiple possible causes including overgrazing and selective feeding of livestock, fire suppression, increases in rainfall and episodically high rainfall, local extinction of mega herbivores, and increasing atmospheric CO_2 concentrations (Roques et al. 2001; Ward 2005; O'Connor et al. 2014). Given the short temporal duration of this study, it is difficult to argue for one or more of these causes. Nevertheless, it is interesting to note that encroachment seems to be confined (with the exception of the anomalous thickening of the SW) to the relatively more mesic eastern parts of the reserve. This pattern reflects what is being found within South Africa, in the sense that more cases of bush encroachment have been documented from mesic areas (O'Connor et al. 2014).

RESTREND and the trend in RUE identified a decreasing trend in vegetation productivity in parts of Gordonia Plains Shrubveld and on dune-slopes in Gordonia Dunveld in the west of TKR. Standardised RESTREND values exhibited a continuous declining trend which suggests that a persistent driver has influenced this pattern. Since these areas have not been burned since 2000 and RESTREND analysis is able to exclude the effect of rainfall on vegetation productivity, the best explanation for the decline in productivity over time is that herbivory has reduced vegetation in these areas.

RESTREND and RUE appear to be useful analytical methods in TKR where erratic rainfall has such a strong influence on annual productivity. However, several limitations in the use of RESTREND have been indicated, such as a reduction in statistical power when shorter periods of time are analysed (e.g. less than 16 growth seasons), and the strong influence of timing on degradation. Wessels et al. (2012) have therefore recommended validating the outcome or simulating the data to test its robustness. This has not been possible in the current study and would be a useful avenue for further research in order to improve confidence in the results.

4.4 Limitations of the Study

The Reliability of the Satellite EO Derived EVI as a Proxy for Plant Productivity

Data derived from MODIS EVI presented biologically meaningful results. The spatial distribution and seasonal variation of EVI showed good accordance with field observation and known phenologies of the plants in the Kalahari. Also, results from this study aligned with those from earlier studies which used time-series MODIS EVI data in the Kalahari (Hüttich et al. 2009; Udelhoven et al. 2015). However, the EVI data derived from Landsat OLI were poorly correlated with vegetation cover values measured in the field, as was also the case in several previous studies which assessed the relationship between vegetation cover and Landsat-derived VI in the Kalahari (Palmer & van Rooyen 1998; van Rooyen 2000; Kong et al. 2015). In this study, with only 18 mm of rain having fallen in the year prior to the field survey, the severe drought experienced by TKR undoubtedly affected both the amount of vegetation cover observed in the field as well as the EVI values as determined from the satellite sensors. Therefore this relationship needs to be re-examined in an appropriate season and year with better rainfall.

Another issue to consider is the possibility that the EVI value could be influenced by vegetation type. For example, the relationship between the EVI value and plant cover estimated in the field in the Koranna-Langeberg Mountain Bushveld demonstrated a substantially different trend from other vegetation types. This difference might be seasonal or due to an unusual response of Koranna-Langeberg Mountain Bushveld to the 2015 drought or due to the topographic effect in rough terrain (Matsushita et al. 2007; Sesnie et al. 2011). Structural and functional trait differences between the plants that comprise different vegetation types, as well as the influence of soil background noise are potential additional explanations for these differences.

Linkage between Plant Productivity and Degradation

Throughout this study, degradation was defined as a change in productivity over time, but this might not equate directly to the process of degradation in the Kalahari. For example, if annuals and perennials demonstrated similar values of productivity in response to rainfall, analytical techniques would not be able to differentiate between degraded areas. In addition, an increase in unpalatable species would also not be indicated by these analyses. For example, field observations confirmed that the density of the unpalatable woody shrub *Crotalaria* sp. was distinctly higher on a livestock farm just outside the boundary fence of TKR, but the difference was not captured by the VI.

Additionally, this study did not distinguish woody and herbaceous components of plant productivity. Therefore, the observed change in plant productivity does not explicitly link to particular growth forms. Several remote sensing studies successfully decomposed woody and herbaceous NDVI signals from time series data using differences in inter-seasonal variation (Lu et al. 2003; Blanco et al. 2016). To understand the extent of potential bush encroachment in the eastern part of TKR, such analytical methods should be employed to further refine the analysis.

Time Frame of the Study

The study period which covered the years 2000-2015 may not be long enough to understand vegetation dynamics in the Kalahari. For example, the maximum number of fires which burned at a location in TKR was only two and it was therefore not possible to make robust assessments of the impact of fire or to evaluate the effects of a change in fire frequency on the vegetation. Additionally, meteorological records indicate that there are rainfall ‘cycles’ in Southern Africa, which involve alternating wet and dry periods at decadal intervals (Thomas & Paul 1991; Mishra et al. 2015a).

Moreover, the process of vegetation recovery from degradation is extremely slow in the Kalahari and does not occur at time scales which are of relevance to the land owner (van Rooyen 2000). For these reasons, a fuller understanding of how the vegetation of the Kalahari responds to rainfall, herbivory and fire will require several decades of data collection.

4.5 Management Implications and Further Research

Based on the findings and limitations of this study the following management implications and future research recommendations are suggested:

1. Bush encroachment was the biggest observed change on vegetation in the past 15 years, with implications for stocking density, animal composition, fire frequencies, and tourism. Further research should aim to evaluate the rate of increase, relative intensity, extent, likely triggers, and possible control measures of bush encroachment in TKR in relation to surrounding areas.

2. The effects of past farming practices were still apparent on vegetation some 20 years after the establishment of TKR, particularly around artificial waterholes and infrastructure. Management practices in the past 15 years have not altered the patterns of plant productivity in these degraded areas suggesting that more proactive management intervention might be required to enable a reversion of these areas to their former state. This result highlighted the sensitivity and irreversibility of severe degradation in the Kalahari environment.

3. Fire was not likely to be a management issue except in the south eastern part of TKR in Koranna-Langeberg Mountain Bushveld, or if actively utilized in order to control woody thickening.

4. The high stocking rates in the Sable and Roan breeding camps have resulted in notable degradation and should be closely monitored in order to prevent an irreversible change in vegetation cover similar to other severely degraded areas in TKR.

5. The change in vegetation productivity outlined in this study needs to be interpreted within the context of longer-term vegetation dynamics in the Kalahari, including the effects of periodic wet and dry spells and extreme episodic events. Historical aerial photographs and Landsat images which extend the time frame of study allow us to answer questions relating to, for example, the impacts of changing land use practices, processes of bush encroachment, and the effects of artificial water points on the vegetation. Such investigations may help to isolate the effects of

past farming practices from more recent impacts caused by reintroduced wildlife or climate change at TKR.

6. The results of RUE and RESTREND need to be verified using satellite images or aerial photographs taken before the year 2000. The areas where changes were indicated should be targeted for further investigation and long-term observation, as well as field based surveys at the species level. These should include demographic surveys of woody shrub species in thicket, and veld condition assessments in more grassy habitats in order to supplement the degradation study.

7. The relationship between VI (including NDVI and EVI) and plant productivity needs to be analysed under different conditions (e.g. soil types, vegetation types and seasons) in the Kalahari to evaluate the potential as well as the limitations of EO derived VI.

5 Conclusions

Using MODIS satellite derived time-series data, an analysis of long-term spatial and temporal change in vegetation productivity was conducted for the 100 000 hectare Tswalu Kalahari Reserve (TKR). Rainfall demonstrated a strong positive correlation with EVI values, a satellite derived indicator of plant productivity, and rainfall was therefore identified as the principal driver of plant productivity in TKR. The relationships between EVI values in individual vegetation types and rainfall as well as phenological and productivity metrics varied, suggesting that differences in species composition, structure and function, and soil type, may have an important influence the EVI values. Fire occurred only infrequently within the Korannaberg Mountains during the recorded period, and its influence on vegetation productivity was therefore considered to be minor.

Results of the RESTREND and RUE analyses suggested that an increase in plant productivity in the woody shrub-dominated vegetation in the eastern and south western parts of TKR may be due to an ongoing process of bush encroachment which browsers are unable to contain. In contrast, vegetation productivity has declined in small areas of Gordonia Duneveld and Gordonia Plains Shrubveld in the western part of TKR, implying possible degradation due to overgrazing. While the drivers of these changes were sometimes difficult to pin down, the extent of degradation within the Roan Sable breeding camps allowed for greater confidence in the speculation that stocking rates in this area are having a notable negative effect on vegetation cover and productivity. However, in all cases verifications of these findings are recommended through field-based monitoring programmes.

The effect on general vegetation productivity of a switch in land-use from livestock farming to a game reserve was not identified. However, field observations indicated severe, spatially discrete degradation in the form of piospheres around historical artificial water points and abandoned infrastructure. These disturbances probably originated in the 1980s, prior to the establishment of the game reserve. These findings indicate that severely degraded areas might not recover without active management intervention, such as have been successfully employ in other arid locations (Carrick & Krüger 2007) .

References

Archibald, S., and R. J. Scholes. 2007. Leaf green-up in a semi-arid African savanna –separating tree and grass responses to environmental cues. Journal of Vegetation Science **18**:583–594.

Baret, F., G. Guyot, and D. J. Major. 1989. TSAVI: a vegetation index which minimizes soil brightness effects on LAI and APAR estimation. Pages 1355–1358 IGARSS'89 and 12th Canadian Symposium on Remote Sensing. Vancouver, Canada.

Bennett, J. E., A. R. Palmer, and M. A. Blackett. 2012. Range degradation and land tenure change: Insights from a "released" communal area of eastern cape province, south africa. Land Degradation and Development **23**:557–568.

Blanco, L. J., Paruelo, J. M., Oesterheld, M., & Biurrun, F. N. 2016. Spatial and temporal patterns of herbaceous primary production in semi-arid shrublands: a remote sensing approach. Journal of Vegetation Science: in press.

Carrick, P. J., and R. Krüger. 2007. Restoring degraded landscapes in lowland Namaqualand: lessons from the mining experience and from regional ecological dynamics. Journal of Arid Environments **70**:767–781.

Childes, S. L. 1988. Phenology of nine common woody species in semi-arid, deciduous Kalahari Sand vegetation. Vegetatio **79**:151–163.

Colditz, R. R., U. Gessner, C. Conrad, D. Van Zyl, J. Malherbe, T. Newby, T. Landmann, M. Schmidt, and S. Dech. 2007. Dynamics of MODIS time series for ecological applications in Southern Africa. Pages 1–6 Proceedings of the 2007 International Workshop on the Analysis of Multi-Temporal Remote Sensing Images. Leuven, Belgium.

Collins, M. et al. 2013. Long-term climate change: projections, commitments and irreversibility. Pages 1029–1136 in T. F. Stocker, D. Qin, G.-K. Plattner, M. Tignor, S. K. Allen, J. Boschung, A. Nauels, Y. Xia, V. Bex, and P. M. Midgley, editors. Climate change 2013: the physical science basis. Contribution of working group I to the fifth assessment report of the Intergovernmental Panel on Climate Change. Cambridge university press, Cambridge, UK and New York, USA.

Collins, S. L. et al. 2014. A multiscale, hierarchical model of pulse dynamics in arid-land ecosystems. Annual Review of Ecology, Evolution, and Systematics **45**:397–419.

Congedo, L. 2013. Semi-Automatic Classification Plugin for QGIS. Available from http://fromgistors.blogspot.com/p/semi-automatic-classification-plugin.html.

Cousins, J., J. Sadler, and J. Evans. 2008. Exploring the role of private wildlife ranching as a conservation tool in South Africa: stakeholder perspectives. Ecology and Society **13**:43.

CSIR. 2012. Soil Type, FUNDISA Disk. Council for Scientific and Industrial Research, Pretoria, South Africa.

Dai, A. G. 2013. Increasing drought under global warming in observations and models. Nature Climate Change **3**:52–58.

Davis, C. 2012. Trends in vegetation productivity and seasonality for Namaqualand, South Africa between 1986 and 2011: an approach combining remote sensing and repeat photography. MSc thesis, Department of Biological Sciences, University of Cape Town, Cape Town, South Africa.

Davis, A. L. V, C. H. Scholtz, U. Kryger, C. M. Deschodt, and W. P. Strümpher. 2010. Dung beetle assemblage structure in Tswalu Kalahari Reserve: responses to a mosaic of landscape types, vegetation communities, and dung types. Environmental Entomology **39**:811–20.

del Barrio, G., J. Puigdefabregas, M. E. Sanjuan, M. Stellmes, and A. Ruiz. 2010. Assessment and monitoring of land condition in the Iberian Peninsula, 1989–2000. Remote Sensing of Environment **114**:1817–1832.

Di Piazza, A., F. Lo Conti, L. V. Noto, F. Viola, and G. La Loggia. 2011. Comparative analysis of different techniques for spatial interpolation of rainfall data to create a serially complete monthly time series of precipitation for Sicily, Italy. International Journal of Applied Earth Observation and Geoinformation **13**:396–408.

Dubovyk, O., T. Landmann, B. F. N. Erasmus, A. Tewes, and J. Schellberg. 2015. Monitoring vegetation dynamics with medium resolution MODIS-EVI time series at sub-regional scale in southern Africa. International Journal of Applied Earth Observation and Geoinformation **38**:175–183.

Eckert, S., F. Hüsler, H. Liniger, and E. Hodel. 2015. Trend analysis of MODIS NDVI time series for detecting land degradation and regeneration in Mongolia. Journal of Arid Environments **113**:16–28.

Eklundh, L., and P. Jönsson. 2012. TIMESAT 3.2 with parallel processing. Available from http://web.nateko.lu.se/timesat/timesat.asp.

Fang, H., S. Liang, M. P. McClaran, W. J. D. Van Leeuwen, S. Drake, S. E. Marsh, A. M. Thomson, R. C. Izaurralde, and N. J. Rosenberg. 2005. Biophysical characterization and management effects on semiarid rangeland observed from landsat ETM+ data. IEEE Transactions on Geoscience and Remote Sensing **43**:125–133.

Fensholt, R., and K. Rasmussen. 2011. Analysis of trends in the Sahelian “rain-use efficiency” using GIMMS NDVI, RFE and GPCP rainfall data. Remote Sensing of Environment **115**:438–451.

Fensholt, R., K. Rasmussen, P. Kaspersen, S. Huber, S. Horion, and E. Swinnen. 2013. Assessing land degradation/recovery in the African Sahel from long-term Earth Observation based primary productivity and precipitation relationships. Remote Sensing **5**:664–686.

Fensholt, R., I. Sandholt, and M. S. Rasmussen. 2004. Evaluation of MODIS LAI, fAPAR and the relation between fAPAR and NDVI in a semi-arid environment using in situ measurements. Remote Sensing of Environment **91**:490–507.

Gillson, L., and M. T. Hoffman. 2007. Rangeland ecology in a changing world. Science **315**:53–54.

Google Inc. 2015. Google Earth. Available from https://earth.google.com/.

Goovaerts, P. 2000. Geostatistical approaches for incorporating elevation into the spatial interpolation of rainfall. Journal of Hydrology **228**:113–129.

Han, J. G., Y. J. Zhang, C. J. Wang, W. M. Bai, Y. R. Wang, G. D. Han, and L. H. Li. 2008. Rangeland degradation and restoration management in China. Rangeland Journal **30**: 233-239

Hempson, G. P., A. W. Illius, H. H. Hendricks, W. J. Bond, and S. Vetter. 2015. Herbivore population regulation and resource heterogeneity in a stochastic environment. Ecology **96**:2170–2180.

Hoffman, M. T., and S. Todd. 2000. A national review of land degradation in South Africa: the influence of biophysical and socio-economic factors. Journal of Southern African Studies **26**:743–758.

Huete, A. R. 1988. A soil-adjusted vegetation index (SAVI). Remote Sensing of Environment **25**:295–309.

Huete, A. R., K. Didan, T. Miura, E. P. Rodriguez, X. Gao, and L. G. Ferreira. 2002. Overview of the radiometric and biophysical performance of the MODIS vegetation indices. Remote Sensing of Environment **83**:195–213.

Hüttich, C., U. Gessner, M. Herold, B. J. Strohbach, M. Schmidt, M. Keil, and S. Dech. 2009. On the suitability of MODIS time series metrics to map vegetation types in dry savanna ecosystems: A case study in the Kalahari of NE Namibia. Remote Sensing **1**:620–643.

Jamali, S., J. Seaquist, L. Eklundh, and J. Ardö. 2014. Automated mapping of vegetation trends with polynomials using NDVI imagery over the Sahel. Remote Sensing of Environment **141**:79–89.

Jeltsch, F., S. J. Milton, W. R. J. Dean, N. Van Rooyen, S. Journal, N. May, J. Suzanne, W. J. Richard, and V. Rooyen. 1997a. Simulated pattern formation around artificial waterholes in the semi-arid Kalahari. Journal of Vegetation Science **8**:177–188.

Jeltsch, F., S. J. Milton, W. R. J. Dean, and N. Van Rooyen. 1997b. Analysing shrub encroachment in the southern Kalahari : a grid-based modelling approach. Journal of Applied Ecology **34**:1497–1508.

Jolly, W. M., and S. W. Running. 2004. Effects of precipitation and soil water potential on drought deciduous phenology in the Kalahari. Global Change Biology **10**:303–308.

Jönsson, P., and L. Eklundh. 2004. TIMESAT—a program for analyzing time-series of satellite sensor data. Computers & Geosciences **30**:833–845.

Kong, T. M., S. E. Marsh, A. F. van Rooyen, K. Kellner, and B. J. Orr. 2015. Assessing rangeland condition in the Kalahari Duneveld through local ecological knowledge of livestock farmers and remotely sensed data. Journal of Arid Environments **113**:77–86.

Lausch, A., M. Pause, I. Merbach, S. Zacharias, D. Doktor, M. Volk, and R. Seppelt. 2013. A new multiscale approach for monitoring vegetation using remote sensing-based indicators in laboratory, field, and landscape. Environmental Monitoring and Assessment **185**:1215–1235.

Lu, H., M. R. Raupach, T. R. McVicar, and D. J. Barrett. 2003. Decomposition of vegetation cover into woody and herbaceous components using AVHRR NDVI time series. Remote Sensing of Environment **86**: 1-18.

Ly, S., C. Charles, and A. Degré. 2013. Different methods for spatial interpolation of rainfall data for operational hydrology and hydrological modeling at watershed scale : a review. Biotechnology, Agronomy, Society and Environment **17**:392–406.

Masunga, G. S., S. R. Moe, and B. Pelekekae. 2013. Fire and grazing change herbaceous species composition and reduce beta diversity in the Kalahari sand system. Ecosystems **16**:252–268.

Matsushita, B., W. Yang, J. Chen, Y. Onda, and G. Qiu. 2007. Sensitivity of the Enhanced Vegetation Index (EVI) and Normalized Difference Vegetation Index (NDVI) to topographic effects: A case study in high-density cypress forest. Sensors **7**:2636–2651.

Mbow, C., R. Fensholt, K. Rasmussen, and D. Diop. 2013. Can vegetation productivity be derived from greenness in a semi-arid environment? Evidence from ground-based measurements. Journal of Arid Environments **97**:56–65.

Mishra, N. B., K. A. Crews, N. Neeti, T. Meyer, and K. R. Young. 2015a. Remote sensing of environment MODIS derived vegetation greenness trends in African Savanna : deconstructing and localizing the role of changing moisture availability , fire regime and anthropogenic impact. Remote Sensing of Environment **169**:192–204.

Mishra, N., K. Crews, J. Miller, and T. Meyer. 2015b. Mapping vegetation morphology types in Southern Africa savanna using MODIS time-series metrics: a case study of central Kalahari, Botswana. Land **4**:197–215.

Mucina, L., and M. C. Rutherford. 2006. The vegetation of South Africa, Lesotho and Swaziland. South African National Biodiversity Institute, Pretoria, South Africa.

Myneni, R. B., R. Ramakrishnan, R. R. Nemani, and S. W. Running. 1997. Estimation of global leaf area index and absorbed par using radiative transfer models. IEEE Transactions on Geoscience and Remote Sensing **35**:1380–1393.

O'Connor, T. G., J. R. Puttick, and M. T. Hoffman. 2014. Bush encroachment in southern Africa : changes and causes. African Journal of Range and Forage Science **31**:67–88.

Ose- Irstea, K. 2015 Geosud Toa Reflectance QGIS plugin. Available from http://equipex-geosud.fr/

Palmer, A. R., and A. Fortescue. 2004. Remote sensing and change detection in rangelands. African Journal of Range & Forage Science **21**:123–128.

Palmer, A. R., I. Samuels, C. Cupido, A. Finca, W. F. Kangombe, I. A. Yunusa, S. Vetter, and I. Mapaure. 2015. Aboveground biomass production of a semi-arid southern African savanna: towards a new model. African Journal of Range & Forage Science:in press.

Palmer, A. R., and A. F. van Rooyen. 1998. Detecting vegetation change in the southern Kalahari using Landsat TM data. Journal of Arid Environments **39**:143–153.

Palmer, A. R., and I. A. M. Yunusa. 2011. Biomass production, evapotranspiration and water use efficiency of arid rangelands in the Northern Cape, South Africa. Journal of Arid Environments **75**:1223–1227.

Parsons, D., C. Shackleton, and R. Scholes. 1997. Changes in herbaceous layer condition under contrasting land use systems in the semi-arid lowveld, South Africa. Journal of Arid Environments **37**:319–329.

Pettorelli, N., J. O. Vik, A. Mysterud, J.-M. Gaillard, C. J. Tucker, and N. C. Stenseth. 2005. Using the satellite-derived NDVI to assess ecological responses to environmental change. Trends in Ecology & Evolution **20**:503–510.

Pfeifer, M., M. Disney, T. Quaife, and R. Marchant. 2012. Terrestrial ecosystems from space: a review of earth observation products for macroecology applications. Global Ecology and Biogeography **21**:603–624.

Reynolds, J., P. Kemp, K. Ogle, and R. Fernández. 2004. Modifying the "pulse–reserve"paradigm for deserts of North America: precipitation pulses, soil water, and plant responses. Oecologia **141**:194–210.

Ringrose, S., and W. Matheson. 1996. The use of integrated remotely sensed and GIS data to determine causes of vegetation cover change in southern Botswana. Applied Geography **16**:225–242.

Roques, K. G., T. G. O'Connor, and a R. Watkinson. 2001. Dynamics of shrub encroachment in an African savanna: relative influences of fire, herbivory, rainfall and density dependence. Journal of Applied Ecology **38**:268–280.

Rutherford, M. C., and L. W. Powrie. 2010. Severely degraded dunes of the southern Kalahari: Local extinction, persistence and natural re-establishment of plants. African Journal of Ecology **48**:930–938.

Rutherford, M. C., and L. W. Powrie. 2013. Impacts of heavy grazing on plant species richness: A comparison across rangeland biomes of South Africa. South African Journal of Botany **87**:146–156.

Sankaran, M. et al. 2005. Determinants of woody cover in African savannas. Nature **438**:846–849.

Scanlon, T. M., J. D. Albertson, K. K. Caylor, and C. A. Williams. 2002. Determining land surface fractional cover from NDVI and rainfall time series for a savanna ecosystem. Remote Sensing of Environment **82**: 376-388.

Schwinning, S., O. E. Sala, M. E. Loik, and J. R. Ehleringer. 2004. Thresholds, memory, and seasonality: understanding pulse dynamics in arid/semi-arid ecosystems. Oecologia **141**:191–3.

Sekhwela, M. B. M., and D. J. Yates. 2007. A phenological study of dominant acacia tree species in areas with different rainfall regimes in the Kalahari of Botswana. Journal of Arid Environments **70**:1–17.

Sesnie, S. E., B. G. Dickson, S. S. Rosenstock, and J. M. Rundall. 2011. A comparison of Landsat TM and MODIS vegetation indices for estimating forage phenology in desert bighorn sheep (Ovis canadensis nelsoni) habitat in the Sonoran Desert, USA. International Journal of Remote Sensing **33**:276–286.

Shongwe, M. E., G. J. Van Oldenborgh, B. J. J. M. Van Den Hurk, B. De Boer, C. A. S. Coelho, and M. K. Van Aalst. 2009. Projected changes in mean and extreme precipitation in Africa under global warming. Part I: Southern Africa. Journal of Climate **22**:3819–3837.

Sjöström, M. et al. 2011. Exploring the potential of MODIS EVI for modeling gross primary production across African ecosystems. Remote Sensing of Environment **115**:1081–1089.

Skarpe, C. 1990. Shrub layer dynamics under different herbivore densities in an arid savanna, Botswana. Journal of Applied Ecology **27**:873–885.

Solano, R., K. Didan, A. Jacobson, and A. Huete. 2010. MODIS Vegetation Index user' s guide (MOD13 Series). Available from http://vip.arizona.edu/documents/MODIS/MODIS_VI_UsersGuide_01_2012.pdf.

South African Weather Service. 2015. Monthly rainfall data. Pretoria, South Africa.

Sporton, D., and D. S. Thomas. 2002. Sustainable livelihoods in Kalahari environments: a contribution to global debates. Oxford University Press, Oxford, UK.

Thomas, D. S. G., M. Knight, and G. F. S. Wiggs. 2005. Remobilization of southern African desert dune systems by twenty-first century global warming. Nature **435**:1218–1221.

Thomas, D. S. G., and H. C. Leason. 2005. Dunefield activity response to climate variability in the southwest Kalahari. Geomorphology **64**:117–132.

Thomas, D. S. G., and A. S. Paul. 1991. The Kalahari environment. Cambridge university press, Cambridge, UK.

Tongway, D. J., A. D. Sparrow, and A. Friedel. 2003. Degradation and recovery processes in arid grazing lands of central Australia. Part 1: soil and land resources. Journal of Arid Environments **55**: 301-326.

Tucker, C. J. 1979. Red and photographic infrared linear combinations for monitoring vegetation. Remote sensing of Environment **8**:127–150.

Udelhoven, T., M. Stellmes, and A. Röder. 2015. Assessing rainfall-EVI relationships in the Okavango catchment employing MODIS time series data and distributed lag models. Pages 225–245 in C. Kuenzer, D. Stefan, and W. Wanger, editors. Remote sensing time series: revealing land surface dynnamics. Springer International Publishing, Cham, Switzerland.

van der Walt, P. T., and E. A. N. le Riche. 1984. The influence of veld fire on an Acacia erioloba community in the Kalahari Gemsbok National Park. Koedoe **27**:103–106.

van Rooyen, A. F. 2000. Rangeland degradation in the southern Kalahari. Ph.D thesis, Department of Range and Forage Science, University of Natal, Pietermaritzburg, South Africa.

van Rooyen, N., D. Bezuidenhout, G. K. Theron, and J. P. Du Bothma. 1990. Monitoring of the vegetation around artificial watering points (windmills) in the Kalahari Gemsbok National Park. Koedoe **33**:63–88.

van Rooyen, N., G. K. Theron, and N. Grobbelaar. 1986. Vegetation of the Roodeplaat Dam Nature Reserve. IV. Phenology an climate. South African Journal of Botany **2**:159–166.

van Rooyen, N., D. van Rensburg, G. Theron, and J. Bothma. 1984. A preliminary report on the dynamics of the vegetation of the Kalahari Gemsbok National Park. Supplement to Koedoe:83–102.

van Rooyen, N., and M. W. van Rooyen. 1998. Vegetation of the South-western arid Kalahari : an overview. Transactions of the Royal Society of South Africa **53**:113–140.

van Rooyen, N., M. W. van Rooyen, and G. J. Bredenkamp. 2005. Vegetation and veld condition in Tswalu Kalahari Reserve. Available from (http://ecoport.org/ep?SearchType_earticleView&earticleId_696&page-2).

von Wehrden, H., J. Hanspach, P. Kaczzensky, J. Fishcher, and K. Wesche. 2012. Global assessment of the non-equilibrium concept in rangelands. Ecological applications **22**:393–399.

Wang, L., P. D'Odorico, S. Ringrose, S. Coetzee, and S. a. Macko. 2007. Biogeochemistry of Kalahari sands. Journal of Arid Environments **71**:259–279.

Ward, D. 2005. Do we understand the causes of bush encroachment in African savannas? African Journal of Range & Forage Science **22**:101–105.

Wasiolka, B., and N. Blaum. 2011. Comparing biodiversity between protected savanna and adjacent non-protected farmland in the southern Kalahari. Journal of Arid Environments **75**:836–841.

Wessels, K. J., S. D. Prince, J. Malherbe, J. Small, P. E. Frost, and D. VanZyl. 2007. Can human-induced land degradation be distinguished from the effects of rainfall variability? A case study in South Africa. Journal of Arid Environments **68**:271–297.

Wessels, K. J., S. D. Prince, and I. Reshef. 2008. Mapping land degradation by comparison of vegetation production to spatially derived estimates of potential production. Journal of Arid Environments **72**:1940–1949.

Wessels, K. J., K. Steenkamp, G. von Maltitz, and S. Archibald. 2011. Remotely sensed vegetation phenology for describing and predicting the biomes of South Africa. Applied Vegetation Science **14**:49–66.

Wessels, K. J., F. van den Bergh, and R. J. Scholes. 2012. Limits to detectability of land degradation by trend analysis of vegetation index data. Remote Sensing of Environment **125**:10–22.

Wistebaar, P. N. 2008. Using remote sensing and expert knowledge to map landscape-level land degradation in the arid grasslands of Bushmanland -South Africa. MSc thesis, Percy FitzPatrick Institute of African Ornithology, University of Cape Town, Cape Town, South Africa.

Appendices

Appendix A The phenometrics quantified by TIMESAT between the 2001-02 and 2014-15 growth seasons.

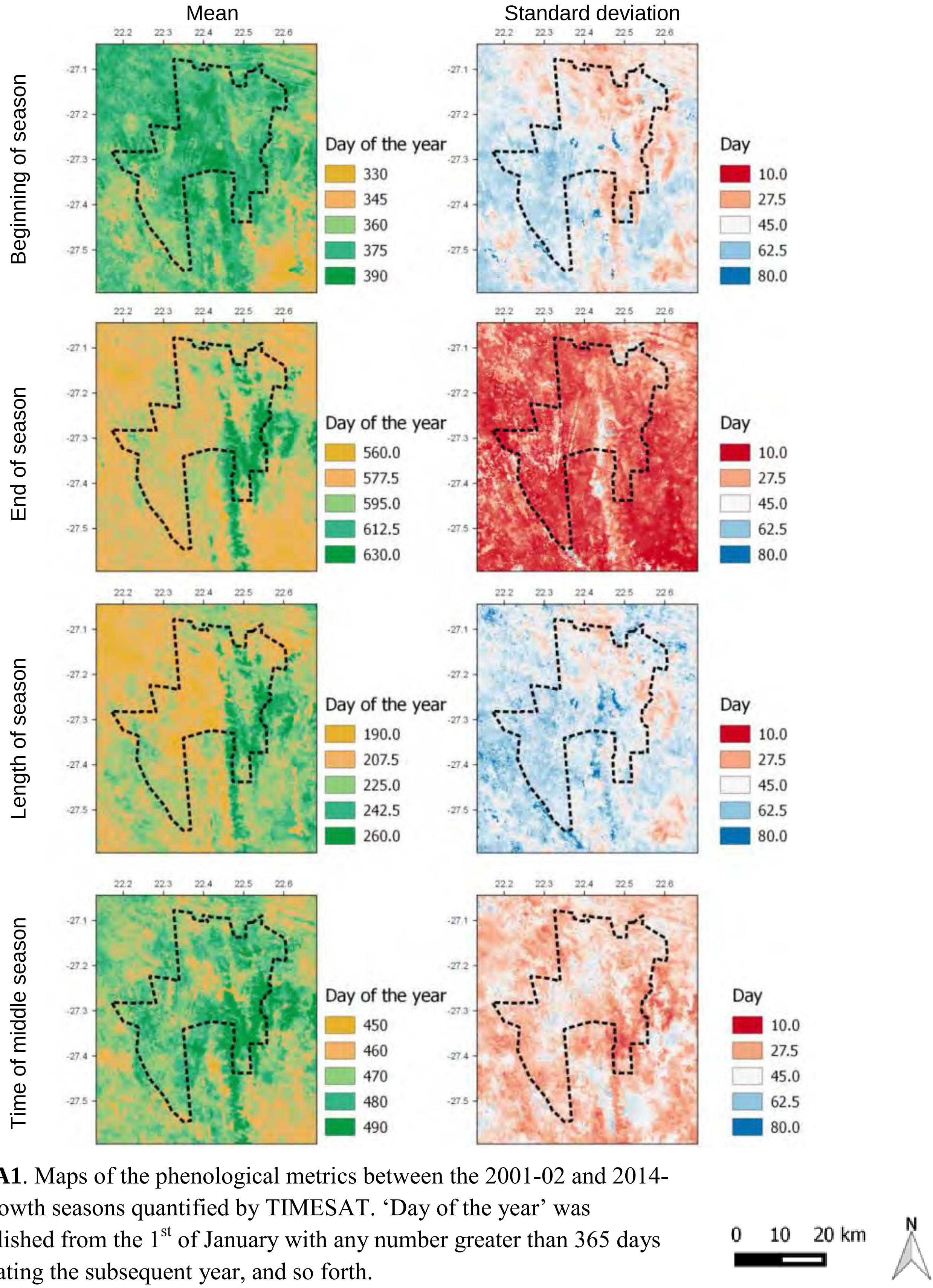

Fig. A1. Maps of the phenological metrics between the 2001-02 and 2014-15 growth seasons quantified by TIMESAT. 'Day of the year' was established from the 1st of January with any number greater than 365 days indicating the subsequent year, and so forth.

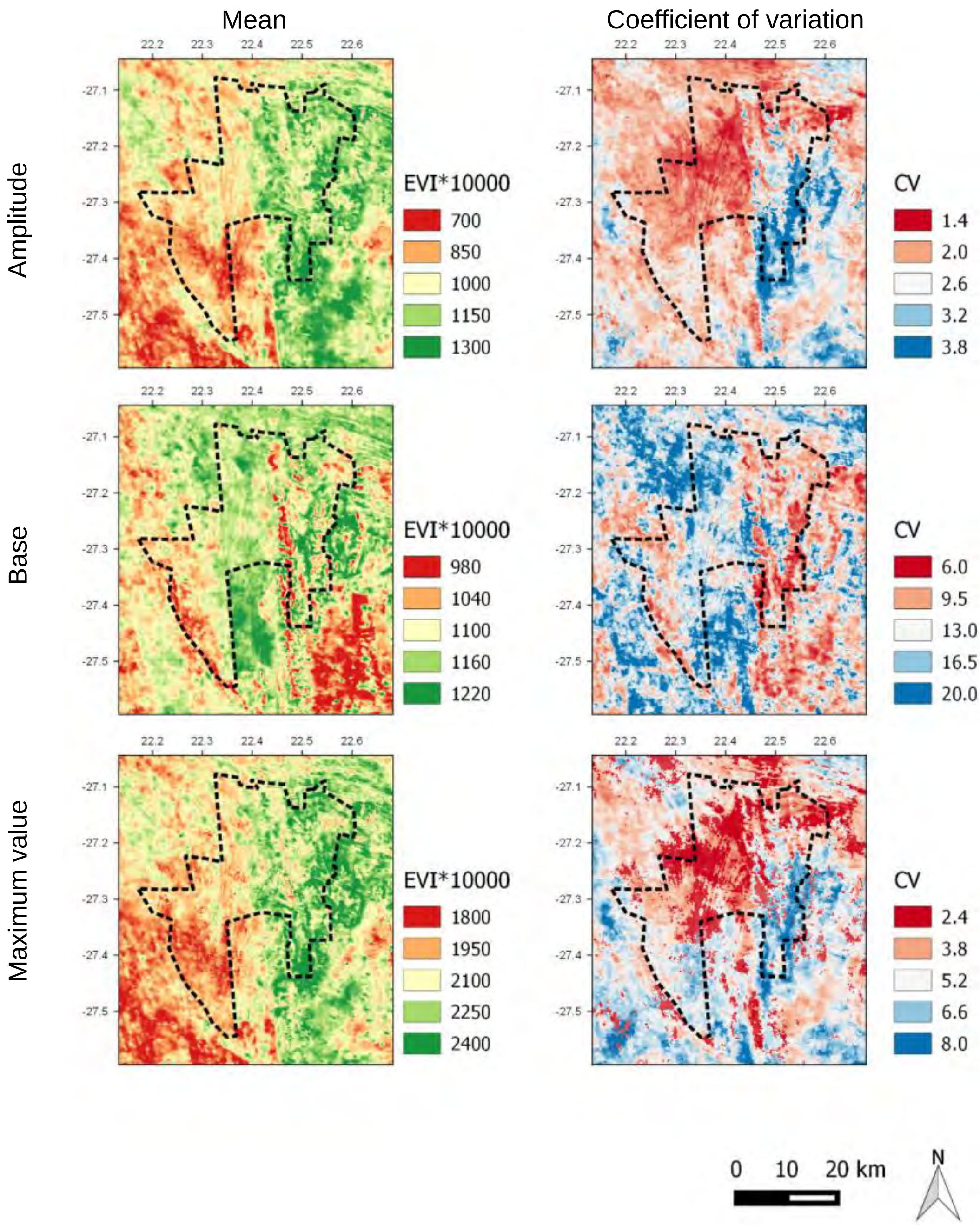

Fig. A2 Maps of the productivity metrics between 2001-02 and 2014-15 growth seasons quantified by TIMESAT.

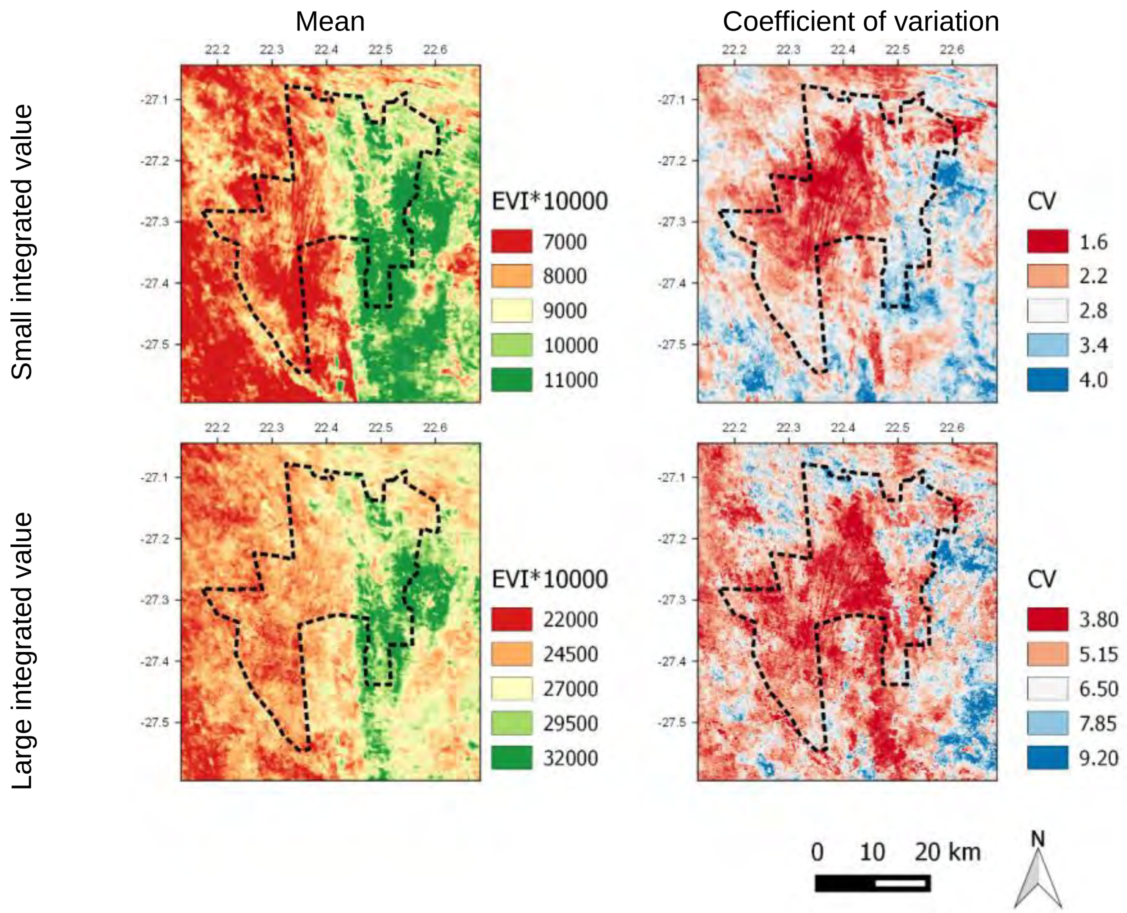

Fig. A3 Maps of the productivity metrics between 2001-02 and 2014-15 growth seasons quantified by TIMESAT.

Table A1 Definitions of the metrics of TIMESAT (after Eklundh & Jönsson 2012 and Wessels et al. 2011). The letters in parentheses corresponds to the key in Fig. 2.3.

Phenology metrics	Productivity metrics
(a) beginning of season; time at which the left edge has increased to a user-defined level (20%) as measured from the left minimum level. (b) end of the season; time at which the right edge has decreased to a user defined level (20%) as measured from the right minimum level. (c) length of season; time from the start to the end of the season. (d) base value; given as the average of the left and right minimum values. (e) time of middle of the season; computed as the mean value of the times for which, respectively, the left edge has increased to the 80 % level and the right edge has decreased to the 80 % level.	(f) maximum value; largest data value for the fitted function during the season. (g) seasonal amplitude; difference between (f) the maximum value and (d) the base value. (h) small integrated value; integral of the difference between the function describing the season and the base level from season start to season end. (h+i) large integrated value; integral of the function describing the season from the season start to the season end. Note that the large integral has no meaning when part of the fitted function is negative.

Table A2 Average $\pm$ standard deviation of phenology and productivity metrics for the 2000-01 - 2014-15 growth seasons computed by TIMESAT for the vegetation types in Tswalu Kalahari Reserve.

	Phenology metrics				Productivity metrics				
Vegetation types	Beginning of season (day of the year)	End of season (day of the year)	Length of season (day)	Time of middle season (day of the year)	Amplitude	Base	Maximum value	Small integrated value	Large integrated value
Koranna-Langeberg Mountain Bushveld	375.5±7.6	624.74± 14.1	249.2± 13.8	489.9± 9.0	0.1164± 0.0108	0.1072± 0.0068	0.2226± 0.0136	1.207± 0.0172	3.091± 0.2470
Gordonia Duneveld	375.4±9.1	583.3±7.2	207.9± 10.3	471.7± 7.0	0.0996± 0.0107	0.1137± 0.0037	0.2099± 0.0123	0.8128± 0.0915	2.530± 0.1456
Gordonia Plains Shrubveld	367.9± 10.8	582.7±7.4	214.8± 11.5	473.6± 6.7	0.0900± 0.0105	0.1085± 0.0046	0.1974± 0.0112	0.7609± 0.0834	2.428± 0.1246
Kathu Bushveld	371.1± 10.1	585.3± 10.1	214.1± 13.0	472.0± 8.1	0.1063± 0.101	0.1120± 0.0047	0.2158± 0.0110	0.8989± 0.0824	2.631± 0.1595
Olifantshoek Plains Thornveld	373.8 ±10.8	592.9± 13.4	219.1± 15.8	475.8± 9.2	0.1173± 0.0103	0.1136± 0.0056	0.2278± 0.0134	1.008± 0.119	2.806± 0.2389

Appendix B Vegetation maps of Tswalu Kalahari Reserve

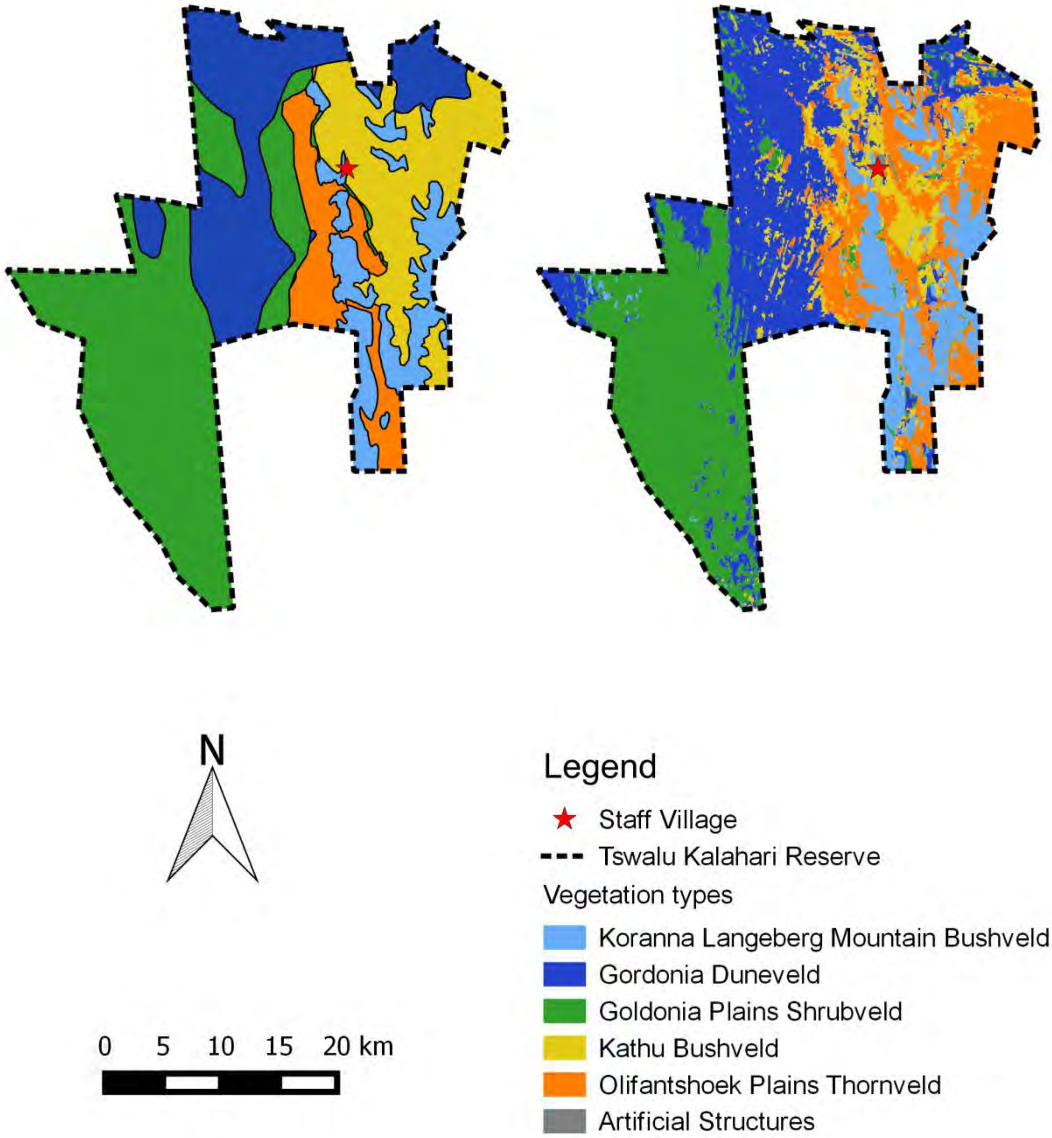

Fig. B1 Comparison of the vegetation maps of Tswalu Kalahari Reserve adapted from Mucina & Rutherford (2006, left) and Landsat-based vegetation map (right)

Appendix C Field survey data

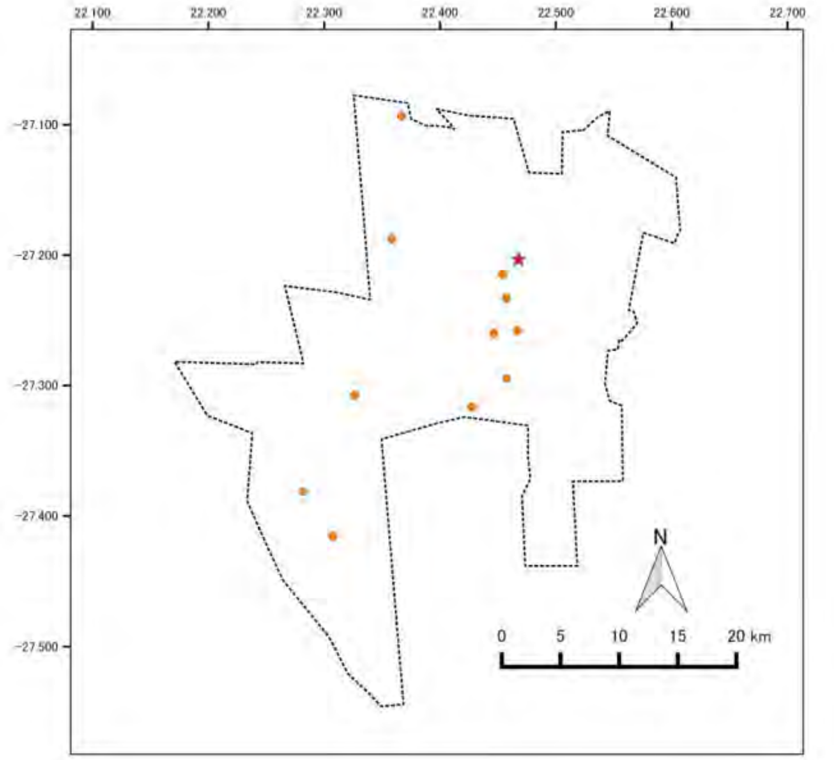

Fig. C1 Locations of the degraded sites (orange dots) in Tswalu Kalahari Reserve (TKR) assessed by field observations in November 2015.

Table C1 Results of transect surveys to test the relationship between Landsat OLI derived EVI values and plant cover in Tswalu Kalahari Reserve. Abbreviations for the vegetation types are as follows: KM = Koranna Langeberg Mountain Bushveld, GD = Gordonia Duneveld, GS = Gordonia Shrubveld, KB=Kathu Bushveld, OT = Olifantshoek Thornveld. Geographical coordinates are shown as decimal degree in WGS 84.

No.	Longitude	Latitude	Vegetation type	EVI	Plant cover (%)					Bare ground (%)		
					Tree	Shrub	Grass	Herb	Sub total	Soil	Rocks	Sub total
1	22.40867	-27.30578	GD	0.138	0.0	5.4	15.1	1.1	21.5	78.5	0.0	78.5
2	22.39781	-27.26121	GD	0.138	0.0	3.2	17.2	3.2	23.7	76.3	0.0	76.3
3	22.40110	-27.23355	GD	0.137	0.0	12.9	8.6	2.2	23.7	76.3	0.0	76.3
4	22.39064	-27.22066	GD	0.147	0.0	9.7	25.8	3.2	38.7	61.3	0.0	61.3
5	22.37847	-27.21617	GD	0.142	0.0	15.1	24.7	1.1	40.9	59.1	0.0	59.1
6	22.34564	-27.23166	GD	0.137	0.0	5.4	16.1	1.1	22.6	77.4	0.0	77.4
7	22.36634	-27.14047	GD	0.140	0.0	26.9	23.7	1.1	51.6	48.4	0.0	48.4
8	22.36246	-27.09555	GD	0.131	0.0	17.2	12.9	6.5	36.6	63.4	0.0	63.4
9	22.39381	-27.13505	GD	0.132	0.0	0.0	32.3	0.0	32.3	67.7	0.0	67.7
10	22.38269	-27.31281	GD	0.142	5.4	9.7	15.1	2.2	32.3	67.7	0.0	67.7
11	22.35786	-27.31522	GD	0.144	0.0	7.5	20.4	2.2	30.1	69.9	0.0	69.9
12	22.31866	-27.48674	GD	0.142	0.0	8.6	29.0	5.4	43.0	57.0	0.0	57.0
13	22.36570	-27.18732	GS	0.161	0.0	36.6	11.8	4.3	52.7	47.3	0.0	47.3
14	22.31987	-27.30773	GS	0.141	5.4	15.1	15.1	0.0	35.5	64.5	0.0	64.5
15	22.31119	-27.31702	GS	0.141	0.0	3.2	16.1	6.5	25.8	74.2	0.0	74.2
16	22.25320	-27.30970	GS	0.148	0.0	23.7	6.5	2.2	32.3	67.7	0.0	67.7
17	22.23088	-27.31992	GS	0.135	0.0	21.5	17.2	0.0	38.7	61.3	0.0	61.3
18	22.22055	-27.31811	GS	0.143	0.0	14.0	9.7	1.1	24.7	75.3	0.0	75.3
19	22.26418	-27.34237	GS	0.139	0.0	21.5	0.0	28.0	49.5	50.5	0.0	50.5
20	22.26670	-27.35020	GS	0.134	0.0	30.1	15.1	1.1	46.2	53.8	0.0	53.8
21	22.28069	-27.37986	GS	0.138	0.0	12.9	23.7	1.1	37.6	62.4	0.0	62.4
22	22.26831	-27.38539	GS	0.136	3.2	4.3	22.6	10.8	40.9	59.1	0.0	59.1
23	22.30091	-27.37073	GS	0.146	4.3	24.7	6.5	1.1	36.6	63.4	0.0	63.4
24	22.30471	-27.38505	GS	0.139	0.0	17.2	32.3	0.0	49.5	50.5	0.0	50.5
25	22.30901	-27.41534	GS	0.142	2.2	17.2	24.7	0.0	44.1	55.9	0.0	55.9
26	22.30464	-27.45654	GS	0.148	0.0	44.1	12.9	0.0	57.0	43.0	0.0	43.0
27	22.30514	-27.47279	GS	0.146	0.0	35.5	26.9	1.1	63.4	36.6	0.0	36.6
28	22.30473	-27.48931	GS	0.147	0.0	22.6	22.6	3.2	48.4	51.6	0.0	51.6
29	22.33536	-27.48631	GS	0.143	0.0	36.6	0.0	11.8	48.4	51.6	0.0	51.6
30	22.35511	-27.43819	GS	0.139	0.0	11.8	35.5	2.2	49.5	50.5	0.0	50.5
31	22.43322	-27.13980	KM	0.094	4.3	28.0	15.1	0.0	47.3	10.8	41.9	52.7
32	22.44170	-27.13998	KM	0.106	0.0	24.7	30.1	1.1	55.9	2.2	41.9	44.1
33	22.44015	-27.13729	KM	0.111	0.0	22.6	25.8	0.0	48.4	8.6	43.0	51.6
34	22.44194	-27.13511	KM	0.113	0.0	10.8	23.7	3.2	37.6	29.0	33.3	62.4
35	22.46232	-27.21262	KM	0.092	0.0	17.2	40.9	0.0	58.1	2.2	39.8	41.9
36	22.45445	-27.21270	KM	0.096	0.0	31.2	26.9	0.0	58.1	1.1	40.9	41.9
37	22.45918	-27.29660	KM	0.129	0.0	28.0	30.1	2.2	60.2	4.3	35.5	39.8
38	22.46099	-27.29604	KM	0.141	0.0	46.2	11.8	1.1	59.1	20.4	20.4	40.9
39	22.46119	-27.28845	KM	0.111	0.0	9.7	16.1	4.3	30.1	20.4	49.5	69.9
40	22.45664	-27.28796	KM	0.106	0.0	20.4	9.7	6.5	36.6	24.7	38.7	63.4
41	22.41330	-27.28840	KB	0.138	0.0	15.1	8.6	2.2	25.8	74.2	0.0	74.2
42	22.41062	-27.17144	KB	0.136	3.2	7.5	16.1	0.0	26.9	73.1	0.0	73.1
43	22.43547	-27.17336	KB	0.137	1.1	3.2	15.1	2.2	21.5	78.5	0.0	78.5
44	22.43117	-27.14470	KB	0.140	0.0	0.0	37.6	0.0	37.6	62.4	0.0	62.4
45	22.46022	-27.19097	KB	0.137	0.0	4.3	50.5	3.2	58.1	41.9	0.0	41.9
46	22.43949	-27.18036	KB	0.139	0.0	12.9	30.1	0.0	43.0	57.0	0.0	57.0
47	22.46671	-27.15462	KB	0.138	4.3	0.0	29.0	2.2	35.5	64.5	0.0	64.5
48	22.44045	-27.23072	KB	0.135	9.7	10.8	14.0	0.0	34.4	65.6	0.0	65.6
49	22.46903	-27.21580	KB	0.137	7.5	11.8	25.8	0.0	45.2	54.8	0.0	54.8
50	22.42208	-27.31133	KB	0.134	0.0	3.2	5.4	6.5	15.1	84.9	0.0	84.9
51	22.41935	-27.31082	KB	0.130	0.0	0.0	10.8	3.2	14.0	86.0	0.0	86.0
52	22.46623	-27.16410	KB	0.144	4.3	0.0	38.7	0.0	43.0	57.0	0.0	57.0
53	22.49120	-27.28813	OT	0.148	0.0	62.4	5.4	0.0	67.7	32.3	0.0	32.3
54	22.49245	-27.29137	OT	0.144	0.0	22.6	4.3	0.0	26.9	73.1	0.0	73.1
55	22.43771	-27.18254	OT	0.142	0.0	19.4	16.1	4.3	39.8	60.2	0.0	60.2
56	22.44766	-27.25014	OT	0.157	5.4	24.7	15.1	0.0	45.2	54.8	0.0	54.8
57	22.44432	-27.24909	OT	0.149	4.3	22.6	9.7	2.2	38.7	61.3	0.0	61.3
58	22.42907	-27.24112	OT	0.134	4.3	26.9	16.1	0.0	47.3	52.7	0.0	52.7
59	22.42696	-27.28935	OT	0.136	0.0	12.9	24.7	0.0	37.6	62.4	0.0	62.4
60	22.50690	-27.30611	OT	0.151	0.0	39.8	8.6	0.0	48.4	51.6	0.0	51.6
61	22.50443	-27.30343	OT	0.144	0.0	60.2	9.7	0.0	69.9	30.1	0.0	30.1
62	22.44726	-27.28914	OT	0.133	0.0	21.5	5.4	1.1	28.0	72.0	0.0	72.0

Appendix D Interpolated rainfall surfaces

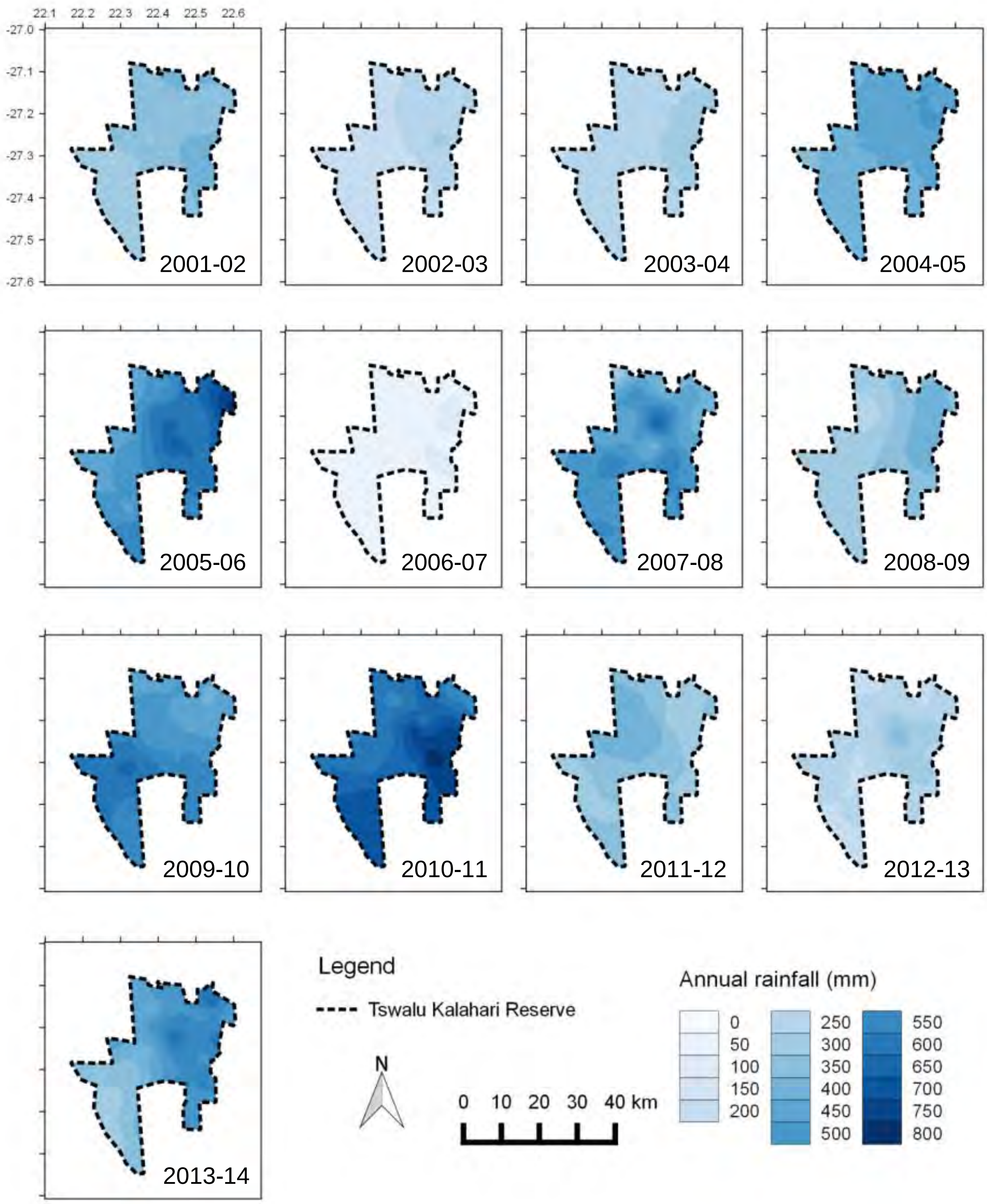

Fig. D1 A composite of interpolated annual rainfall surface contour maps computed by ordinarily kriging for the growth seasons (October - September) in Tswalu Kalahari Reserve.

Appendix E Degradation trend analysis

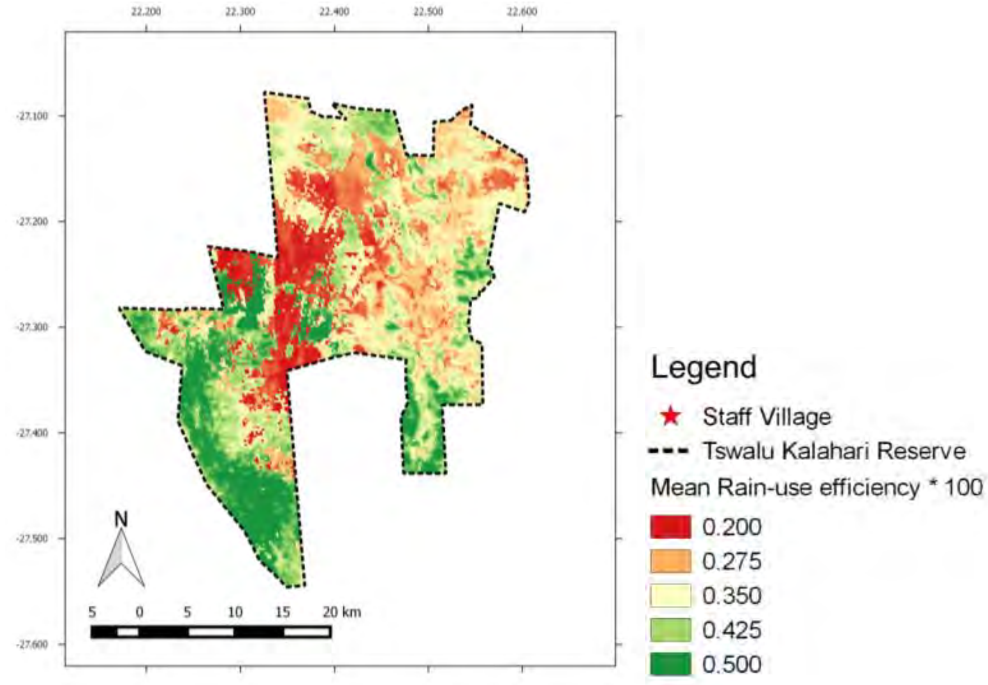

Fig. E1 Mean of relative rain use efficiency (RUE) in Tswalu Kalahari Reserve between 2001-02 and 2013-14 growth seasons, including the drought season of 2006-07. High RUE values (green) indicate higher efficiency and a decrease in this efficiency is assumed to occur in association with land degradation.

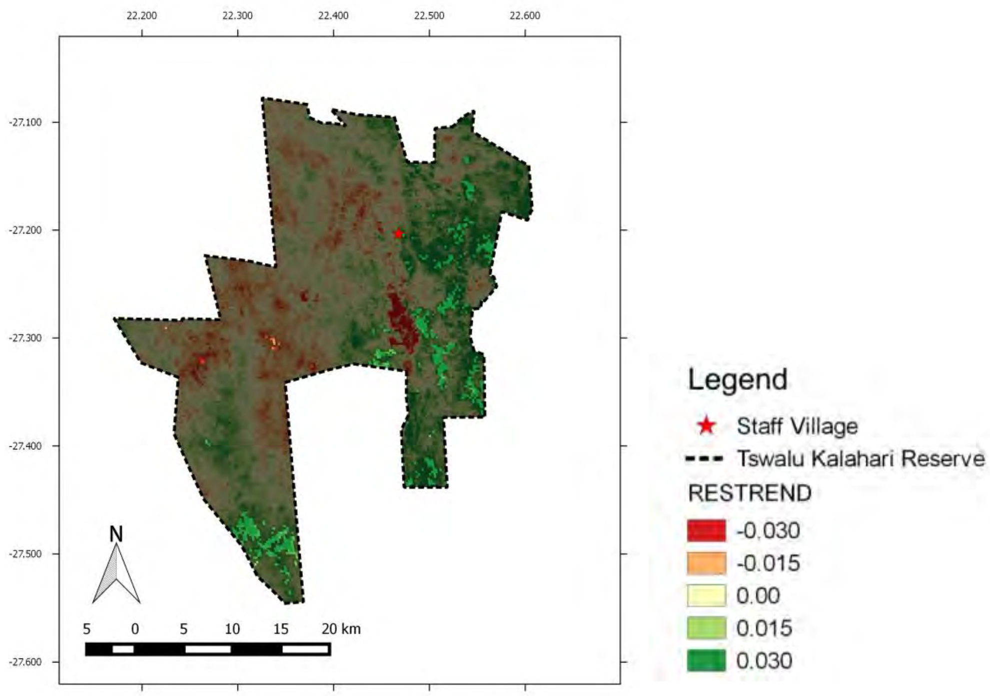

Fig. E2 Slope of the regression analysis of RESTREND including the drought season of 2006-07. Areas where significant trends were not found were displayed as the grey shaded colour.

Appendix F Past and current Landsat images

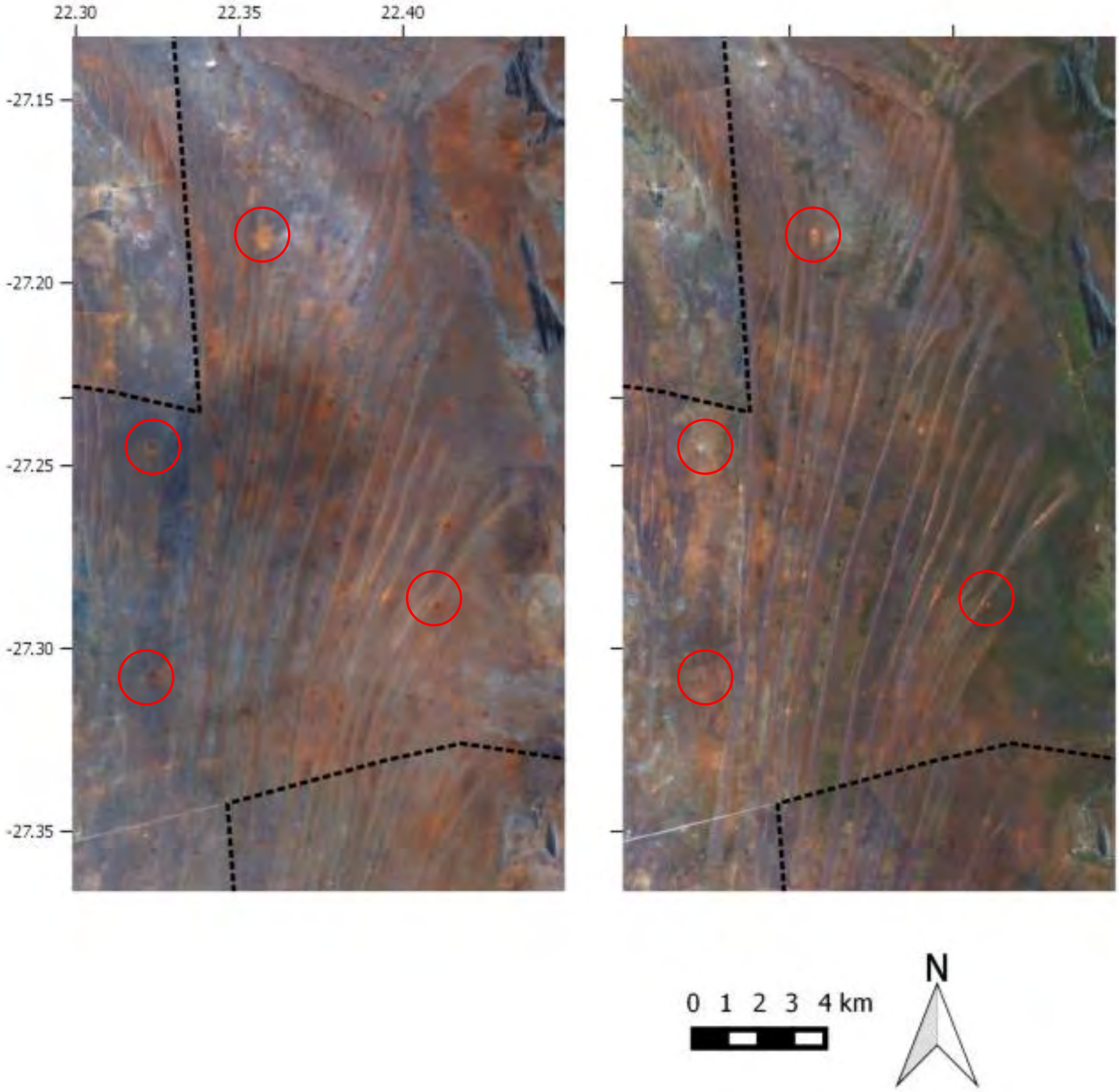

Fig. F1 Comparisons of true colour satellite images from Landsat TM and OLI obtained at different times in the central part of Tswalu Kalahari Reserve. The image on the left was obtained in 19 March 1989 and the image on the right was taken on 02 April 2014. Both images show a piosphere effect around artificial water points (indicated with red circles), suggesting that the effect was initiated before the area became a game reserve.